CORNELL UNIVERSITY

Center for Radiophysics and Space Research

ITHACA, N. Y.

CRSR 792

Production and Condensation of Organic Gases In the Atmosphere of Titan

Carl Sagan
W. Reid Thompson

Laboratory for Planetary Studies
Cornell University
Ithaca, NY 14853

Production and Condensation of Organic Gases
In the Atmosphere of Titan

Carl Sagan
W. Reid Thompson

Laboratory for Planetary Studies
Cornell University
Ithaca, NY 14853

ABSTRACT

The rates and altitudes for the dissociation of atmospheric constituents on Titan are calculated for solar ultraviolet radiation, the solar wind, Saturn magnetospneric particles, the Saturn co-rotating plasma, and cosmic rays. Laboratory experiments show that a variety of simple gas phase organic molecules and more complex organic solids called tholins are produced by such irradiations of simulated Titanian atmospheres. Except for ultraviolet wavelengths longward of the methane photodissociation continuum, most dissociation events occur between about 3100 and 3600 km altitude, corresponding well to the region of EUV opacity detected by Voyager. For a wide variety of simple to moderately complex organic gases in the Titanian atmosphere, condensation occurs below the top of the main cloud deck at about 2825 km. We propose that such condensates, beginning with CH_4 at about 2615 km, comprise the principal mass of the Titan clouds. There is a distinct tendency for the atmosphere of Titan to act as a fractional distillation device, molecules of greater complexity condensing out at higher altitudes. To produce the observed detached limb hazes near 2900 km by the condensation of such organic gases, the rate at which abundance falls with increasing heavy atom number, n, should lie between about $10^{-0.25n}$ and about $10^{-0.5n}$, just the range suggested by laboratory experiments. There seem to be no plausible circumstances in which such hazes will condense in observable abundances at optical frequencies at altitudes much above the observational upper limit of 3000 km. Typical organic

compounds which condense out at the 2900 km level are in the molecular weight range 100 to 150 daltons. Organic molecules produced or condensed at higher altitudes have properties similar to the so-called "Axel dust." There should be a sedimentary column of condensed organic ices and tholins on the surface of Titan, produced by coagulation and sedimentation of cloud and haze particles; the depth of this layer, accumulated over 4.5×10^9 years, ranges from about 100 meters (if only $\lambda <$ 1440 Å photons can photodissociate atmospheric constituents) to kilometers (if considerably longer wavelength ultraviolet photons can be employed with quantum yields ~ 0.1.)

Introduction

It has long been known, since Kuiper's (1944) spectroscopic discovery, that Titan holds a reducing atmosphere composed at least in part of the simplest organic molecule, methane (see also Trafton, 1972). Subsequent photometric and polarimetric observations indicated a very red, ultraviolet-absorbing material (Harris, 1961; see also Caldwell, 1974), probably distributed in and above a thick cloud deck (Veverka, 1973; Zellner, 1973). Knowing that photolysis of CH_4 alone leads to a range of complex hydrocarbons, and that dissociation of CH_4 and other cosmically abundant reduced compounds leads to dark red organic heteropolymers (Khare and Sagan, 1973), it was natural to suggest that the clouds of Titan might be composed, at least in part, of complex organic molecules (Sagan, 1971; 1973; 1974; Khare and Sagan, 1973). The quantities of organic molecules synthesized on Titan over geological time were estimated to be at least hundreds of g cm^{-2} (Sagan, 1974; Chang _et al_., 1979).

The hypothesis of abundant organic matter in the atmosphere of Titan was supported by the identification of infrared emission features (Gillett _et al_., 1973) with the hydrocarbons C_2H_2, C_2H_4, and C_2H_6 in a Titanian atmospheric inversion (Danielson _et al_., 1974). The Voyager infrared spectrometer experiment (Hanel _et al_., 1981; Maguire _et al_., 1981; Kunde _et al_., 1981) clearly established the presence of aliphatic hydrocarbons up to C_3, substituted and polyacetylenes, and nitriles. The results are summarized in Table 1. Additionally, most of these gas phase organics have been produced in laboratory experiments by sparking, electron-irradiating or ultraviolet-irradiating a mixture of N_2 and CH_4 in approximately the Titan atmospheric proportions (Balestic, 1974; Toupance _et al_., 1975; Raulin _et al_., 1979; Gupta _et al_., 1981).

Ultraviolet, infrared, imaging, and radio occultation experiments, conducted during the Voyager 1 and 2 encounters with Titan in November 1980 and August 1981, revealed a deep N_2/CH_4 atmosphere overlying a surface at 2575 km and 94 K (Hanel et al. 1981; Tyler et al. 1981; Broadfoot et al. 1981); with a thick, opaque and nearly featureless cloud deck extending to about 2825 km, and distinct limb hazes above the main cloud deck at altitudes ranging to about 2925 km (Smith et al. 1982a; Rages, 1983). Haze layers merge with the main cloud deck toward Titan's north pole, with separation increasing toward the south and with multiple haze layers apparently present at high southern latitudes (Smith et al. 1981, 1982a).

The availability of a nominal pressure-temperature profile for Titan's atmosphere based on Voyager radio occultation and IRIS experiments (Hanel et al. 1981; Tyler et al. 1981; Samuelson et al. 1981), and of more detailed information on high-energy charged particles in Saturn's magnetosphere has prompted us to investigate the altitude-specific deposition of energy by those sources thought to be responsible for most of the organic synthesis on Titan: solar ultraviolet radiation, the solar wind, Saturn magnetospheric high energy particles, Saturn corotating plasma, and solar and galactic cosmic rays. It will then be possible to consider the rate of organic synthesis on Titan, and the possible condensation of synthesized molecules to form the observed clouds and haze.

Energy Sources

(1) Solar Ultraviolet Light

Methane is photolyzed at $\lambda < 1440$ Å and nitrogen at $\lambda < 800$ Å. The solar UV photon flux is taken from the compilation of Heroux and Hinteregger (1978), the N_2 absorption spectrum from Allen (1965), and the CH_4 absorption spectrum from Okabe and Becker (1963) and from Koch and Skibowski (1971). Photon deposition as a function of altitude is computed by numerical integration of the CH_4 and N_2 absorption, employing the nominal Voyager pressure-temperature profile. Minor atmospheric constituents, including those in Table 1 and those discussed below, will increase the photon deposition rates. In this and other computations, the model (p,T) profile is represented as a grid of (p,T) points recorded at a resolution of 0.01 in $\log_{10}p$, with an assumed linear temperature gradient between the grid points. The pressure-altitude scale is generated from this profile by a seminumerical solution of the equation of hydrostatic equilibrium. Photodissociation rates are computed initially assuming unit quantum yield for photolysis, and zero quantum yield at $\lambda > 1440$ Å.

(2) Magnetospheric high energy particles.

Saturn magnetosphere high energy particle fluxes were measured by Voyagers 1 and 2 (Krimigis et al. 1981, 1982). We assume negligible intrinsic or induced magnetic field strength for Titan. Levels of energy deposition for charged particles are then computed from semi-empirical relationships (Cook et al. 1953; Friedlander et al. 1964) to determine the penetration loading density L (g cm^{-2}), and thus the effective pressure level of penetration $p = \bar{\mu}gL/\mu X$, for protons having the measured energies. Since the Voyager results are reported only for energy intervals, and since for protons of energies E less than several hundred MeV nearly all the particle energy is deposited near the penetration level, altitude limits for energy deposition are determined by calculating the penetration level of particles at the minimum and maximum extremes of the reported range. The number of dissociations per unit volume for this altitude range is then $N = r\Omega E/\epsilon d\Delta z$, where r is the counting rate (units, s^{-1}); d is the detector factor [0.12 cm^2 sr for Voyager detectors (Krimigis et al. 1977)]; Ω is the detector acceptance solid angle (assumed to be 2π); ε is the net particle energy required per dissociation, taken as 10 eV [the bond strength of N_2 is 9.9 eV; of CH_4, 4.5 eV]; and Δz is the altitude range.

Saturn magnetospheric particle fluxes are summarized in Table 2. The computed dissociation rates, if based only on particle counting rates near $20R_s$ in the magnetopause at spacecraft entry (about 14° and 8° from the noon meridian for Voyagers 1 and 2, respectively), would be substantial overestimates, since particle fluxes near $20R_s$ at spacecraft exit (about 137° and 93°, respectively, from the noon meridian) are reduced by factors of 10 to 100 (cf. Table 2). [This is the reason that our magnetospheric fluxes and (below) dissociation rates are significantly less than those of Strobel (1982).] Planetary magnetocentric approach angles are taken from Ness et al. (1981, 1982). We estimate, based on this sparse information, that Titan spends roughly 1/4 of its orbit in the region of high particle flux; peak dissociation rates are scaled accordingly to give net dissociation rates. Because the flux in the lowest energy range measured is still substantial near the noon meridian, there may be significant but periodic additional dissociation caused by < 28 keV protons at high altitudes.

(3) Solar Wind

Although Titan's orbit is usually contained completely within Saturn's magnetosphere, this was not the case at the Pioneer 11 [CHK] encounter (van Allen et al., 1980). Titan is estimated to lie beyond the magnetopause, exposed to the solar wind, about 20% of the time (Bridge, 1981). The solar wind at Saturn has a density of about 0.1 cm^{-3}, at velocities of 450 to 550 km s^{-1}, and a random-kinetic temperature of about $10^{4.8}$K (Wolfe et al., 1980). The solar wind energy deposition occurs primarily between the penetration levels of 450 and 550 km s^{-1} (1.05 keV to 1.57 keV) protons.

(4) Corotating plasma

Another source of charged particles in the upper Titanian atmosphere is plasma corotating with Saturn's magnetic field. At Titan's distance from Saturn, the plasma lags the magnetic field: a rotational velocity of about 150 km s^{-1}, a density of 0.1 cm^{-3}, and a random kinetic temperature of 5×10^5K were indicated by the Voyager plasma analyzers (Bridge et al., 1981, 1982). A Maxwell-Boltzmann energy distribution is computed and vectorially added to the measured rotational energy (∿ 120 eV per particle) to produce the net energy distribution used to determine altitudes of plasma energy deposition. The vertical resolution in this computation is about 35 km.

(5) Cosmic rays

The final energy source we consider is solar and galactic cosmic rays. Low-energy cosmic ray altitude-specific dissociation rates were computed by digitizing the measured cosmic ray spectrum at the Earth (Biswas and Durgaprasad, 1979), finding penetration depths as for Saturn magnetospheric particles, and computing the flux in a given energy range deposited in the altitude interval between the maximum and minimum penetration depths. For higher energy cosmic rays (>500 MeV), the results of Capone et al. (1980) were employed.

Dissociation and Synthesis Rates.

Dissociation rate per unit volume from all five sources is shown as a function of altitude in Figure 1. For the solar wind, the endpoints of the vertical line represents the limits of the altitude interval over which the given average dissociation rate applies. The total altitude-integrated dissociation rates are displayed in Table 3.

Above the main cloud deck, Saturn magnetospheric particles and solar UV are the dominant energy sources. The solar wind and the Saturn corotating plasma also make significant contributions, but over much more restricted altitude intervals; the total dissociation rate is much smaller for these sources (cf. Table 3). Neglecting the possibility that long wavelength ultraviolet photons can be employed through photolysis of minor constituents, the highest dissociation rates are at 3100 to 3700 km altitudes, well above the clouds and visible hazes. The contribution of solar H Ly α radiation is localized near 3400 km. Significant CH_4 dissociation, by those wavelengths closest to the dissociation threshold of 1440 Å, continues down to about 3040 km. Cosmic rays are deposited mainly in the main cloud deck in the altitude range 2600 to 2750 km.

For high energy charged particles, we assume ∿ 1 dissociation of an atmospheric molecule per 10 eV deposited along each ion track through the Titanian atmosphere. For direct CH_4/N_2 photolysis we assume unit quantum yield and (cf. Strobel, 1974; Allen <u>et al</u>., 1980) unit efficiency in the production of heavier organics. It is also possible that $\lambda > 1440$ Å ultraviolet radiation can be effective in indirect methane photodissociation and in the production of higher molecular weight organic molecules. A small steady state abundance of such long-wavelength absorbers as H_2S, NH_3, and aldehydes can, on photodissocation , generate superthermal hydrogen atoms which in turn provide the activation energy for subsequent chemical reactions (Sagan and Khare, 1971a, 1971b, 1974). Small quantities of NH_3 may exist in the Titanian atmosphere and the detection of CO_2 well above the clouds (Maguire, et al., 1982) suggests that small quantities of the simplest aldehydes should be present there as well. Precisely because of their large ultraviolet absorption cross-sections the abundances of such molecules should be low.

The resulting surface deposit of complex organic compounds from each energy source, accumulated over 4.5 x 10^9 years, is also given in Table 3. These molecules are not expected to be merely such simple gas phase organics as are detected spectroscopically (Table 1), but also a category of complex organic heteropolymers called tholins that are produced by high-energy irradiation of simulated Titanian atmospheres and that seem to reproduce well the observed spectral properties, particle sizes, and refractive indices of the clouds of Titan (Sagan and Khare, 1981, 1983; Khare et al., 1981). Scanning electron microscopy of tholins (Sagan and Khare, 1981) shows no significant void volume and implies a density ~ 1 g cm^{-3}. Thus the numbers in the last column of Table 3 are also the anticipated thicknesses (in cm) of accumulated tholin sediment on the surface of Titan from the various energy sources listed. We see that a layer at least 100 meters thick is expected and, if wavelengths longer than 2000 Å are utilized with production quantum yields larger than 0.1, depths of kilometers seem possible.

The likelihood that tholin densities are ~ 1 g cm^{-3} implies, for the Toon et al. (1980) model of coagulation and sedimentation in the Titanian clouds, an organic production rate $\sim 3.5 \times 10^{-13}$ g cm^{-2} sec^{-1}, corresponding to a column of tholin $\sim$ 0.5 km thick built up over geological time. This in turn implies (cf. Table 3) that wavelengths longer than the onset of the methane photodissociation continuum near 1440 Å are being utilized for photochemistry on Titan, and perhaps provides some evidence for long-wavelength-absorbing organic intermediaries producing hot hydrogen atoms. If, for example, the mean molecular weight of organic products produced by a single long wavelength photolytic event were $\mu = 30$ with an effective quantum yield of 0.1, wavelengths as long as about 2200 Å would have to be employed; equivalently, for $\mu = 30$ and an effective quantum yield of 10^{-2}, wavelengths as long as 2600 Å would be required. We stress, however, that the conclusions of this paragraph are highly model-dependent.

Cloud and Haze Condensation Processes.

All significant energy deposition occurs at least 100 km above the highest optical hazes at about 2900 km, except for the cases of long-wavelength UV, and cosmic rays where the energy is deposited in and below the main cloud deck. Thus (again excepting long-λ UV) the largest part of organic synthesis in the Titan atmosphere takes place at high altitudes; the region of the optical hazes and upper main cloud deck is in fact a deep minimum in the dissociation/synthesis rate curve, indicating that the presence of well-defined haze layers near 2900 km is not the result of local primary production of organic molecules. If hot-hydrogen photochemistry occurs in the 2825 to 2925 km region, it is utilizing long-wavelength photon acceptors probably produced at higher altitude.

In a solar occultation experiment, the Voyager 1 ultraviolet spectrometer detected (Broadfoot et al., 1981; Smith, et al., 1982b) an absorbing layer in the 1540 to 1630 Å bandpasses at an altitude of 3250 to 3600 km. It corresponds to no known optical haze layer, and is believed due to atomic or molecular absorption. This is just the region of maximum direct methane photolysis (Figure 1). While methane is transparent at 1540 - 1630 Å, ethane, propane, butane, and higher paraffin hydrocarbons begin absorbing significantly (Okabe and Becker, 1963), as do many other organic molecules. (This ultraviolet opacity through the upper atmosphere of Titan is responsible in part, through the absorption of sunlight, for the essentially isothermal regime at about 160°K which extends from below the main cloud deck to the exobase.) The picture suggested is that significant dissociation of major atmospheric constituents occurs between 3100 and 3700 km, where the products constitute an organic haze, contributing to the UV but not to the visible opacity -- because of *in situ* production, not necessarily because of vapor condensation. Below 3100 km, the situation may be reversed.

In early irradiations of CH_4/N_2 atmospheres, performed in the context of the origin of life, high molecular weight products up to some 900 daltons were detected (Balestic, 1974). In proton bombardment experiments, aliphatic hydrocarbons up to C_{22} have been reported (Scattergood and Owen, 1977). Pyrolytic GC/MS of the solid organic tholins produced on sparking methane/ammonia mixtures detects some 50 compounds (Khare _et al._, 1981). Preliminary pyrolytic GC/MS analysis of tholins prepared in a Titan atmosphere simulation indicates a comparable or greater variety and complexity (Khare _et al._, 1982). The Titan tholins, which match the observed properties of the Titan clouds (Sagan and Khare, 1981, 1982; Khare _et al._, 1981), presumably form from simpler constituents resembling their pyrolyzates, and release their pyrolyzates on irradiation. Thus, with a wide variety of simple and complex organic molecules expected in the atmosphere of Titan, each characterized by its own vapor pressure curve, we anticipate condensation at many levels in the Titanian atmosphere. Do the condensation levels correspond to the observed altitudes of the main cloud layer and the detached limb hazes?

Since the suite of organic gases detected in the Titan atmosphere is still only a tiny fraction of the gases likely to be present, we need to estimate the rate at which molecular abundance falls with increasing heavy atom number, a parameter whose common logarithm we define as α. In Figure 2 we have plotted, from various simulation experiments and from measurements of terrestrial organic sediments, the relative mole fraction of organics versus the heavy atom (C or N) number. The slope of these curves yields α. Also plotted is a segment of the observed curve for Titan (Table 1). There are no Voyager measurements for butane or higher paraffin hydrocarbons on Titan and it is not yet appropriate to consider the butadiyne or cyanoacetylene abundances as representative of the abundance of molecules with four heavy atoms in the Titan atmosphere. We see from Figure 2 that ultraviolet irradiation at

$\lambda < 1440$ Å, and electrical discharge or high-energy electron bombardment of methane or methane/nitrogen mixtures at a wide variety of pressures yields a value of $\alpha \approx 0.25$ to 0.5. Suspected abiogenic hydrocarbon gases dissolved at great depth in Black Sea sediments give α between 0.3 and 1.0 (Hunt and Whelan, 1978). Only the Nonesuch shale hydrocarbons, which are probably biogenic, have values of α significantly less than in simulation experiments, at least in the low heavy-atom number range. The currently available data make the observed value of α for Titan comparable to that in laboratory simulations; comparable values emerge from an elaborate absolute reaction rate kinetics calculation of Titanian photochemistry (Yung, 1982). Pyrolyzates of CH_4/NH_3 tholins produced by long-wavelength ultraviolet or spark irradiation exhibit compounds with up to nine heavy atoms present at an abundance about 10^{-1} to 10^{-2} that of the most abundant pyrolyzates (Khare et al., 1978, 1981); i.e., tholin pyrolyzates exhibit values of α almost as small as for the Nonesuch shale. Similar conclusions apply for CH_4/N_2 tholins (Khare et al., 1982). Despite our sense from these data that $0.25 \leq \alpha \leq 0.5$, we do not deduce from Figure 2 any particular value of α for the atmosphere of Titan, and the calculations below are performed for $\alpha = 1.0$, 0.5, 0.25, and 0.

To test the hypothesis that organic products in detectable abundances might condense at the altitudes of the observed clouds or hazes, vapor saturation curves have been constructed for the Voyager-detected molecules (Hanel et al., 1981; Maguire et al., 1981; Kunde et al., 1981); for some of the major and minor tholin pyrolyzates of synthesis experiments for which extensive gas chromatographic/mass spectrometric analysis has been performed

(Khare et al., 1981); and for a series of aliphatic hydrocarbons and aromatic ring systems. The estimated abundances are given by $X = X_0 \, 10^{-\alpha(n - n_0)}$, where X is the mole fraction, n is the heavy atom number, and the zero subscript denotes the reference molecule. For each class of molecule, the reference was that Voyager-detected molecule judged most appropriate: for saturated hydrocarbons, C_3H_8; for alkenes, C_2H_4; for alkynes and aromatic rings, C_2H_2; for saturated nitriles, HCN; for dinitriles, C_2N_2; etc. Molecules exhibiting more than one functionality were generally assigned the smallest abundance calculated for each functionality independently. For $\alpha = 0$, X was calculated assuming constant weight fraction rather than mole fraction as a function of n.

Saturation curves were constructed using data from various sources (e.g., Weast, 1980), employing standard values for heats of vaporization and fusion and at least one pressure-temperature reference point. In a single case, cyanoacetylene, the heat of vaporization, and in some cases, the heat of fusion, was estimated by comparison with a series of homologous compounds because relevant data could not be found in the literature (Appendix I). The normal hydrocarbon and aromatic series were chosen as models largely because of the readily available vapor pressure data. Variation of the heats of vaporization and fusion with temperature was generally unavailable, and in any case is of insufficient magnitude to be of concern here. Condensation temperatures T_c as a function of atmospheric pressure p are given by

$$T_c = [T_r^{-1} - \frac{R/\mu}{\Delta H} \ln \frac{pX}{p_r}]^{-1}$$

where T_r and p_r constitute a vapor pressure-temperature reference point, R is the universal gas constant, μ is the molecular weight, ΔH the heat of vaporization or sublimation, as appropriate, and X the mole fraction. (When the vapor pressure is below the triple point pressure, the computed temperature will be below the freezing point, and the heat of sublimation, which is the sum of the heats of vaporization and fusion, is used.) Condensation occurs when the curve so constructed intersects the atmospheric structure curve ($T_c \geq T_{atm}$).

Figure 3 exhibits vapor pressure curves for all the Voyager-detected organic compounds; every one of them condenses out below the upper reaches of the main cloud deck ($\cong$ 2825 km). Since CH_4 condenses at about 2615 km and all detected compounds condense below 2700 km, the upper portion of the main cloud deck must consist almost entirely of higher molecular weight molecules, both the organic condensates discussed here and tholins.

Vertical optical depths, τ_v, of particulate condensates of detected compounds are estimated from the scattering cross-section, κ, in the geometric limit:

$$\tau_v = \frac{\mu X \kappa p}{\bar{\mu} g} = \frac{3 \mu X p}{2 \bar{\mu} g \rho r}$$

where ρ and r are particle density and radius. For altitudes near 2900 km ($g - 107$ cm s^{-2}),

$$\tau_v = 1.4 \times 10^6 \, (\mu/\bar{\mu}) X p_{mb}$$

for particles of $\rho \sim 1$ g cm^{-3} and $r \sim 0.1$ μm (anticipating smaller particles at higher altitudes; cf. Toon _et al_., 1980). At these altitudes, if the particle and gas scale heights are comparable, the air mass for tangential observations is about 20. A value of τ_v as small as 5×10^{-2} suffices to generate unit tangential optical depth in the condensate haze. It is clear that even minor constituents of the region below about 3500 km can produce large optical depths of condensate: vertical optical depths computed for condensation of Voyager-detected compounds are displayed in Table 4. Within the main cloud deck, some tens of kms above the CH_4 condensation level, there are optically very thick pure scattering clouds of ethane and propane.

There is a very simple constraint on the altitude of the highest possible detectable haze: for condensation processes in which the abundance falls at least fast enough that the mass fraction is constant with molecular weight ($\mu X/\bar{\mu}$ = constant $\leq 10^{-5}$), a tangential optical depth ~ 1 implies $p \geq 10^{-2}$ mb. Thus no optically observable hazes should exist above about 3000 km. In fact 3000 km is very close to the altitude of the highest detected hazes at visible wavelengths (Smith <u>et al</u>., 1982a; Rages and Pollack, 1983). The visible-wavelength reflectivity of Titan would be much greater than it is if these large optical depths of non-absorbing ice hazes surmounted the main cloud deck. But even for $\alpha = 0$, it is very difficult to arrange $\tau_v >> 1$ above 2900 km, and no contradiction with observation emerges.

Figures 4a-d show the condensation levels for normal hydrocarbons with various values of α, the index of the (assumed constant) decrease of abundance with molecular weight. Using these aliphatic hydrocarbons as a model series, we see that observable hazes at the correct altitudes can be produced provided $\alpha \leq 0.5$. The substantial optical depth of the main cloud deck below 2775 km also requires a decrease no faster than this. No compounds condense in adequate abundance to produce visible wavelength opacity above about 2670 km -- i.e., anywhere in the upper clouds -- if $\alpha \geq 1$ (Figure 4d .

The results for a similar model based on representative aromatic ring systems are shown in Figures 5a-d. If the production of higher molecular weight products is extensive (Figure 5a-b), compounds condensing below about 3000 km can be seen; but those having more than about 10 heavy atoms, both for the aliphatic series, Fig. 4a-b, and the aromatic series, Fig. 5a-b, will condense at higher altitudes -- many at the level of production -- and be mixed vertically as particulates rather than as gases. Members of the model ring series have a lower overall abundance since the reference molecule adopted for this computation is C_2H_2. For this series, the generation of observable hazes at high altitudes requires $\alpha \lesssim 0.25$ (Figure 5b).

In Figures 6 a-d are shown vapor pressure curves for a few of the most abundant tholin pyrolyzates made in simulation experiments (Khare, et al., 1981). These low molecular weight compounds condense at altitudes below 2700 km, in the main cloud deck. In order for them to contribute significant cloud opacity there, α must be ≤ 0.5. Results for some lower abundance GC/MS tholin pyrolyzates are shown in Figures 7a-d. Again, if these compounds are to produce substantial opacity in and possibly above the main cloud deck, α must be ≤ 0.5. (A small laboratory value of α is indicated by the simple fact that these pyrolyzates can be detected at all by GC/MS.)

Conclusions.

Many of the molecules produced in greatest abundance in Titan's upper atmosphere condense at the level of the main cloud deck. Discrete hazes may be produced by the condensation of a single major compound, or of a group of compounds which condense at approximately the same altitude. Nearly all high molecular weight products synthesized at high altitude will condense in situ.

In all cases for which detectable hazes condense near 2900 km altitude, the heavy atom number appears to be around 9 or 10, and we are led to speculate that the detached limb hazes are composed of molecules with approximately this number of (carbon plus nitrogen) atoms. The condensation of molecules with a particular number of heavy atoms at a particular altitude derives from a general correlation between molecular weight and vapor pressure curve, a correlation which is remarkably similar for many different categories of organic molecules. Thus, because of its temperature structure, the atmosphere of Titan serves as a kind of fractional distillation device, condensing out simple organic molecules deep below the cloudtops, molecules of intermediate complexity near the cloudtops, and detached hazes and molecules of still greater complexity at higher altitudes -- where their number density is too low to be detected optically, but where they may contribute to the observed opacity in the extreme ultraviolet. To explain the detached limb hazes by such a fractional distillation/condensation mechanism requires, for most categories of molecules tested, that $\alpha \leq 0.5$. This is just the range suggested by the relevant laboratory simulation experiments in which methane or methane/nitrogen mixtures are irradiated (Fig. 2), and suggests that the detached hazes may in fact be organic condensates in the molecular weight range 100 to 150 daltons.

The highest measured instantaneous particle fluxes from the Saturn magnetosphere (Table 2) are a factor $\geq$ 4 greater than the adopted mean values in Table 3. Accordingly, those particle fluxes may periodically produce incremental dissociation rates a few tens of percent that produced by the most abundant indisputable energy source, the methane photodissociation continuum and H Ly α in the solar ultraviolet. Thus, it seems possible that the Titanian atmosphere and clouds exhibit, superposed on longer-term variations (Sromovsky, et al., 1981), a brightness or color variability with a period equal to the Titan orbital period, or to half that period.

We recognize at least three varieties of organic hazes or clouds in the atmosphere of Titan: (1) primary production hazes of simple organic molecules chiefly in the 3200 to 3600 km range; (2) condensation hazes of primary production organic molecules chiefly localized in the detached limb hazes below 2900 km and in the main cloud deck; and (3) tholins, formed from the irradiation of atmospheric constitutents and chemical reaction of primary hazes, chiefly localized in the main cloud deck below 2800 km. In addition, some in situ generation and substantial reprocessing of organic hazes by near-UV radiation may occur in the few scale heights near and above the tops of the visible clouds. The condensation of methane at about 2615 km is probably responsible for the minimum near that altitude in the atmospheric temperature structure curve (cf. Fig. 3). These organic condensations are generally entirely transparent in the visible (although much less so in the middle ultraviolet), and through pure multiple scattering would diffuse and render indistinguishable Titanian surface contrast, even if there were no pure absorption by the tholin particles. The scattering optical depths for propane, ethane, and especially methane, may be enormous (cf. Table 4). The properties of the high-altitude hazes -- including substantial ultraviolet opacity and negligible visible absorption (although providing significant scattering) -- are consistent with the so-called "Axel dust" proposed for the upper atmosphere of Titan (Danielson, 1974), as well as for Jupiter (Axel, 1972) and Saturn (Macy, 1973). We will report in a separate communication on the application of similar ideas to Jupiter and Saturn.

Ultraviolet irradiation of organic ices at 77K leads to significant radical mobility and the synthesis of organic molecules of greater complexity (Khare and Sagan, 1973). The longer an alkane is, the longer the wavelengths to which its ultraviolet absorption extends (Okabe and Becker, 1963). Aromatic rings characteristically absorb to 2600 Å and longer. With, say, a 10-yr residence time above the main cloud deck for 0.3 μm particles (cf. Toon et al., 1980) the accumulated ultraviolet dose by such hazes for $\lambda < 2000$ Å amounts to the breaking of every chemical bond several times over, assuming an effective quantum yield, $\phi \sim 0.1$. (The same is true at $\lambda < 1440$ Å for $\phi \sim 1$.) Eventually -- for example, through the production of polyenes, or porphyrins, or polyaromatics -- the condensates that originally had substantial opacity only in the ultraviolet, begin to darken in the visible as well. It is possible that ultraviolet-damaged organic condensates are, on Titan, an alternative path to the synthesis of tholins.

The main cloud deck must be at least somewhat differentiated, with products of lower volatility and/or higher abundance condensing in its upper reaches, and those of higher volatility and/or lower abundance condensing at lower altitudes. The higher molecular weight products condensing at higher altitudes will precipitate through and to some degree be mixed with generally more abundant condensates at lower altitudes. The mix of condensed ices and largely photoproduced tholins, coagulating and sedimenting out of the Titanian atmosphere will provide a rich layer of complex organics at the surface. Further processing of organic sediments on the Titanian surface by cosmic rays (cf. Fig. 1) is expected despite the low ambient temperatures.

Acknowledgments.

We thank M. Nowak for help in compiling data used in our vapor pressure computations, and B.N. Khare and Y. Yung for helpful discussions. This research was supported by NASA grants NGR 33-010-082 and NGR 33-010-101.

Appendix I

The following estimates of heats of fusion were made from homologous compounds:

Formula	Name	ΔH_f, cal g^{-1}
CH_2CHCN	acrylonitrile	40
CH_3CH_2CN	propanonitrile	35
C_4H_8	1-butene	30
C_4H_8	cis-2-butene	30
C_4H_8	trans-2-butene	30
$(CH_2CN)_2$	succinonitrile	35
ϕCN	benzenonitrile	32
$CH_3\phi C_2H_5$	3-ethyltoluene	26
C_4H_9CN	pentanonitrile	28
$CH_3\phi CN$	p-tolunitrile	32
C_6H_{12}	1-hexene	30
$\phi CHCH_2$	styrene	32
$CH_3CHCHCN$	methacrylonitrile	35
CH_2CH_2	ethylene	33
CHCCN	cyanoacetylene	40
$\phi CH_2\phi$	diphenylmethane	30
ϕ_3CH	triphenylmethane	30
$n\text{-}C_{13}H_{28}$	---	35.8
$n\text{-}C_{14}H_{30}$	---	53.4
$n\text{-}C_{15}H_{32}$	---	37.5
$n\text{-}C_{16}H_{34}$	---	55.6
$n\text{-}C_{17}H_{36}$	---	39.1
$n\text{-}C_{26}H_{54}$	---	39.

Heats of fusion for linear hydrocarbons were derived by linear interpolation between the nearest available values for odd or even carbon number representatives, as appropriate -- a permissible approach because of the smooth variation of the heats of fusion of the odd and even carbon number series, taken independently. For other molecules, we employed the heats of fusion of those compounds, for which data were available, that were chemically and structurally most similar. These values were adjusted in some cases to take account of trends in the heats of fusion of a structurally similar series. E.g., we adopt

$$\Delta H_f(n\text{-}C_8H_{16}) \approx \Delta H_f(n\text{-}C_6H_{12}) + [\Delta H_f(n\text{-}C_8H_{18}) - \Delta H_f(n\text{-}C_6H_{14}).$$

Table 1

Identified and Deduced Constituents of the Atmosphere of Titan
(Hanel, *et al.*, 1981; Maguire, *et al.*, 1981;
Kunde, *et al.*, 1981; Maguire, *et al.*, 1982; Yung, 1982)

N_2	Nitrogen	81-93%
[^{36}Ar	Argon	≈ 12% ?]
CH_4	Methane	≈ 6%
[Ne	Neon	< 1%]
H_2	Hydrogen	≈ 0.2%
CO	Carbon monoxide	≈ 0.1%
$HC\equiv CH$	Acetylene	2 ppm
$H_2C=CH_2$	Ethylene	0.4
H_3C-CH_3	Ethane	20
$H_3C-CH_2-CH_3$	Propane	3
$HC\equiv C-C\equiv CH$	Butadiyne (Diacetylene)	0.03
$H_3C-C\equiv CH$	Methylacetylene	0.03
$HC\equiv C-C\equiv N$	Cyanoacetylene	0.1-0.01
$HC\equiv N$	Hydrogen cyanide	0.2
$N\equiv C-C\equiv N$	Cyanogen	0.1-0.01
CO_2	Carbon dioxide	0.01 ppm

Table 2

Saturn Magnetospheric Particle Flux Measurements
(Calculated from the Voyager measurements of Krimigis, *et al*., 1981, 1982)

Energy Range keV	Meridian	Counts/sec	Intensity $cm^{-2}\ s^{-1}\ sr^{-1}$	Flux $eV\ cm^{-2}\ s^{-1}$	Spacecraft
28 - 43	0	600.	5×10^3	1.1×10^9	V2
	90	20.	1.7×10^2	$4. \times 10^7$	V2
53 - 85	0	200.	1.7×10^3	$8. \times 10^8$	V1
	140	30.	$2. \times 10^2$	1.1×10^8	V1
80 - 137	0	600.	$5. \times 10^3$	$4. \times 10^9$	V2
	90	7.	$6. \times 10^1$	$4. \times 10^7$	V2
220 - 540	0	100.	$8. \times 10^2$	1.9×10^9	V2
	90	0.3	2.	$6. \times 10^6$	V2
550 - 1050	0	0.2	2.	$8. \times 10^6$	V1
	140	0.1	0.8	$4. \times 10^6$	V1
990 - 2100	0	0.2	2.	1.9×10^7	V2
	90	0.04	0.3	$3. \times 10^6$	V2

Table 3

Net Dissociation and Synthesis Rates*

Energy Source	Dissociation Rate cm^{-2} sec^{-1}	Synthesis Rate of Organic Molecules $g\ cm^{-2}/4.5 \times 10^9$ yr
UV, $1450 \geq \lambda \geq 800$ Å (CH_4 dissociation)	3.6×10^9	1×10^4
UV, $\lambda < 800$ Å (N_2 dissociation)	2.8×10^8	760
Solar Wind	3.2×10^7	90
Saturn Magnetosphere Particles	1.9×10^8	540
Saturn Corotating Plasma	8.0×10^6	22
Cosmic Rays	1.0×10^8	290
[UV, $\lambda <$ 2000 Å ($\phi \sim 0.1$)	3.4×10^9	9700]
[UV, $\lambda <$ 2500 Å ($\phi \sim 0.1$)	3.2×10^{11}	9×10^5]

*Except for the last two rows, we assume 1 dissociation per 10 eV for charged particles, 1 dissociation per photon for UV, and a net yield of 1 carbon or nitrogen atom incorporated into organic products per dissociation. For longer wavelength UV, we tentatively adopt a quantum yield for higher organics ~ 0.1. Because products are expected to have densities ~ 1 g cm^{-3}, the last column also gives the depth in cm of organic sediments accumulated on its surface over the history of Titan.

Table 4

Optical Depths for Condensates of Known Atmospheric Constituents*

Compound	Vertical Optical Depth
HC_3N	20.
HCN	5.
C_4H_2	25.
C_2N_2	28.
C_3H_8	1200.
C_3H_4	2.
C_2H_2	80.
C_2H_6	1300.
C_2H_4	770.

*Compounds are listed in condensation sequence from higher to lower altitudes (Figure 3). Listed values assume the presence of an amount of condensate equal to the column abundance of the overlying vapor. Actual optical depths will depend on atmospheric settling and mixing rates, and on actual particle sizes (assumed here to be ∿ 0.1 μm).

Figure Captions

Figure 1: Variation of dissociation rate with altitude for various energy sources at Titan. Assumed dissociation efficiencies are one per 10 eV for charged particles and one per photon for $\lambda < 1440$ Å UV. For illustration we include two points, representing the photolysis of hypothetical minor atmospheric constituents at $\lambda < 2000$ Å and at $\lambda < 2500$ Å -- in both cases assuming a photodissociation cross-section $\sim 10^{-18}$ cm^2 and a mole fraction $X \sim 10^{-7}$. If not for the presence of the clouds and limb haze these near UV photodissociation events would happen roughly at 2625 km, near the peak dissociation level for cosmic rays.

Figure 2: The abundance of simple organics (mainly, normal hydrocarbons) as a function of heavy atom number for a variety of laboratory simulation experiments, terrestrial biogenic and suspected abiogenic sediments, and for Titan. The slope of these curves yields the abundance parameter α, used to calculate Figs. 4-7. Sample values of α are shown in the inset.

Figure 3: Vapor saturation temperature profiles for Voyager-detected organic molecules in Titan's atmosphere. On each curve is shown the generic formula, name and abundance of the condensate. All compounds condense in the mid- to lower clouds, below 2660 km. Condensation of C_2H_4 is marginal.

Figures 4a-d: Vapor saturation temperature profiles for normal hydrocarbons up to C_{26}. Abundances are based on C_3H_8 at 2×10^{-5} mole fraction. Calculations are performed for four values of α, the rate at which abundance decreases for each increment in heavy atom number. Detectable condensates at the altitudes of observed hazes and the upper cloud can be formed only for $\alpha \leq 0.5$.

Figures 5a-d: Vapor saturation temperature profiles for representative aromatic ring systems. Abundances are based on C_2H_2 at 2 x 10^{-6} mole fraction. Detectable hazes require $\alpha \leq 0.25$.

Figures 6a-d: Vapor saturation temperature profiles representative of abundant tholin pyrolyzates detected by GC/MS after a CH_4/NH_3 laboratory simulation experiment (Khare et al., 1981). Similar products result from CH_4/N_2 simulations (Khare et al., 1982). Condensation occurs in the main cloud deck for all abundance models.

Figures 7a-d: Vapor saturation temperature profiles for representative minor pyrolyzates detected by GC/MS after a CH_4/NH_3 laboratory simulation experiment (Khare et al., 1981). Similar products result from CH_4/N_2 simulations (Khare et al., 1982). Condensation of detectable amounts of organic products at the altitudes of the hazes and upper cloud deck occurs only if $\alpha \leq 0.25$. The condensation of a few particularly abundant compounds could result in thin haze layers, as observed.

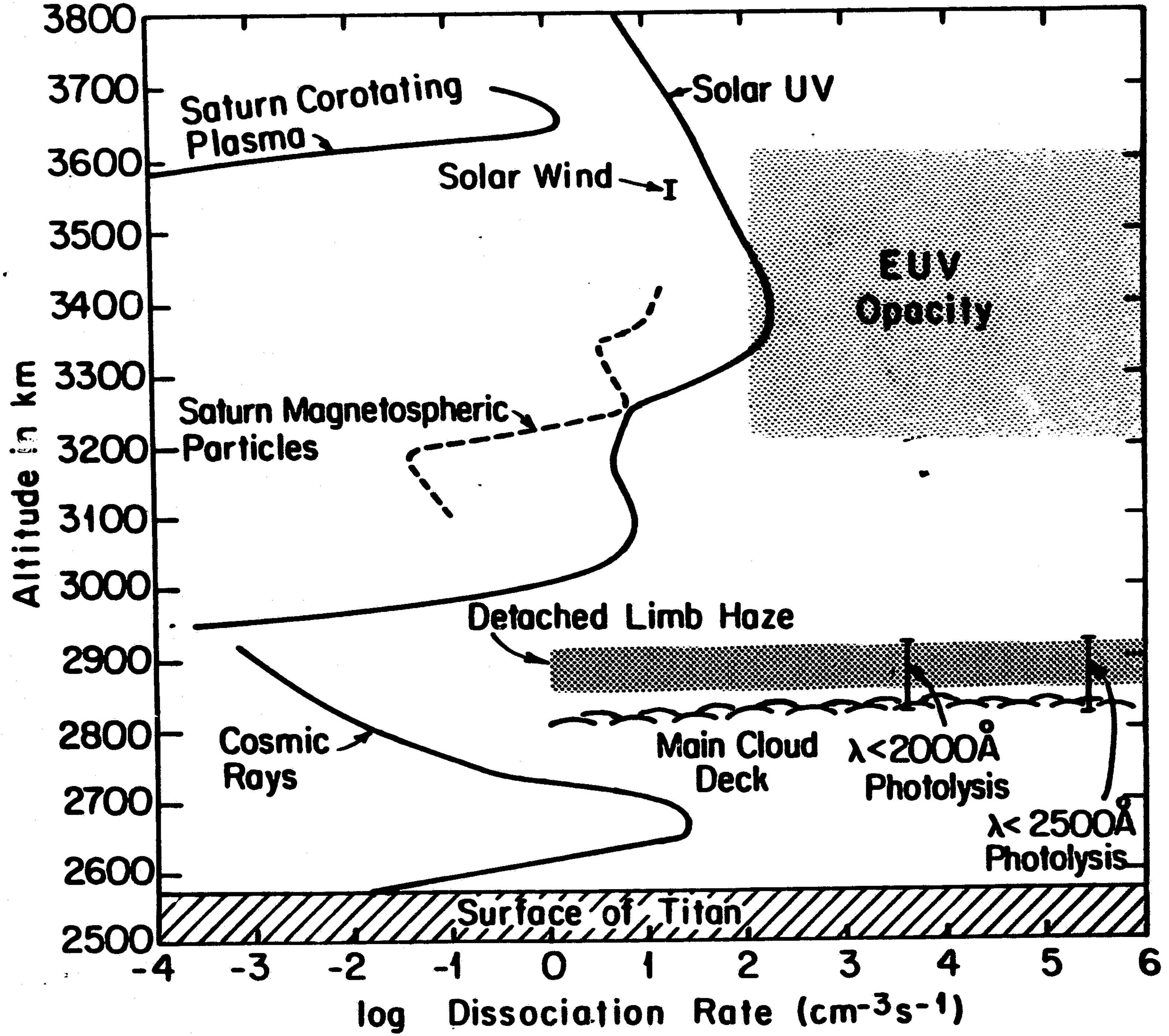
3800
3700
3600
3500
3400
3300
3200
3100
3000
2900
2800
2700
2600
2500
Altitude in km
-4
-3
-2
-1
0
1
2
3
4
5
6
log Dissociation Rate ($cm^{-3}s^{-1}$)
Saturn Corotating Plasma
Solar UV
Solar Wind
EUV Opacity
Saturn Magnetospheric Particles
Detached Limb Haze
Cosmic Rays
Main Cloud Deck
λ<2000Å Photolysis
λ< 2500Å Photolysis
Surface of Titan

Figure 1

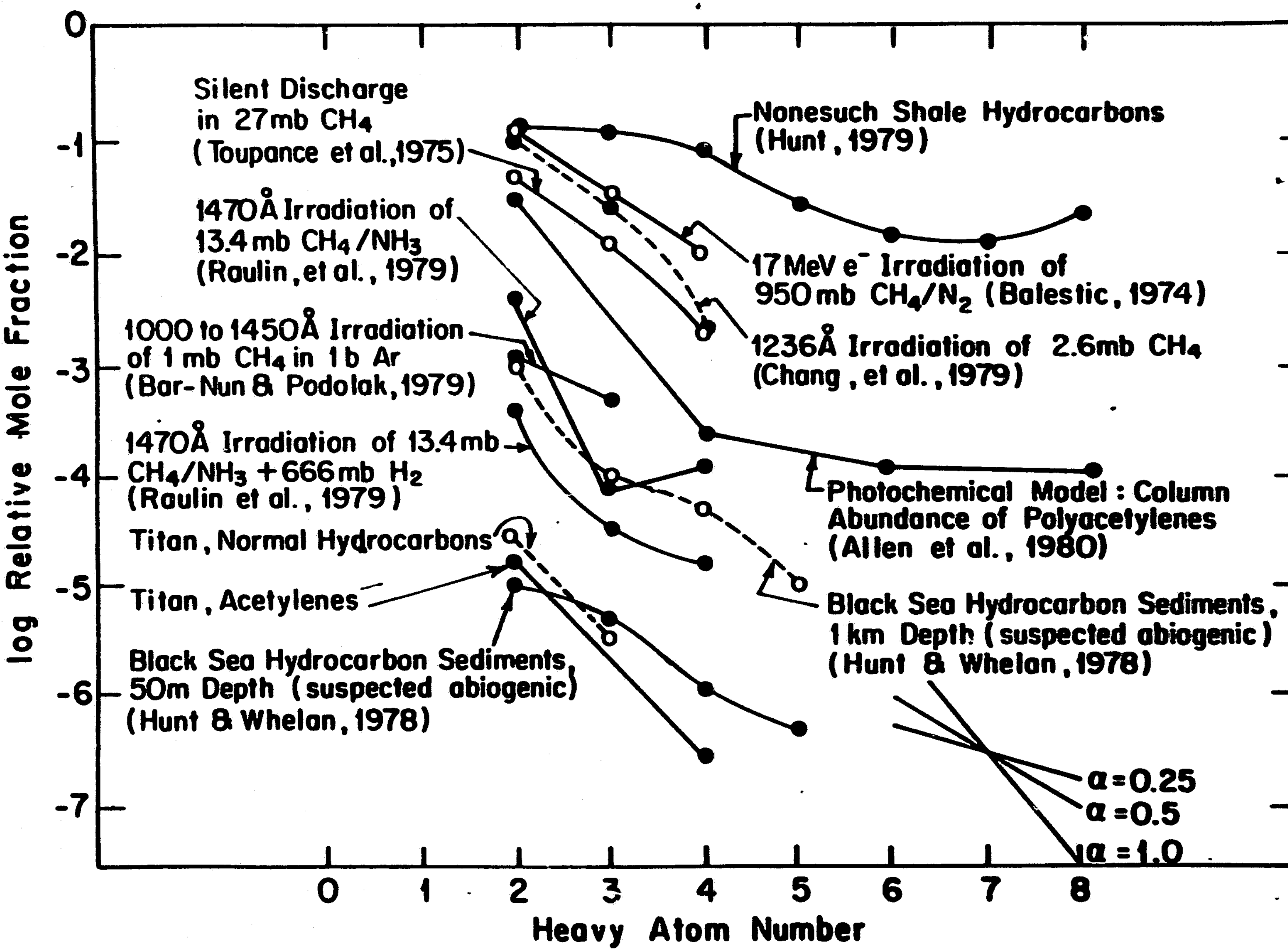
0
-1
-2
-3
-4
-5
-6
-7
log Relative Mole Fraction
0
1
2
3
4
5
6
7
8
Heavy Atom Number
Silent Discharge in 27mb CH_4 (Toupance et al.,1975)
1470Å Irradiation of 13.4mb CH_4/NH_3 (Raulin, et al., 1979)
1000 to 1450Å Irradiation of 1 mb CH_4 in 1 b Ar (Bar-Nun & Podolak, 1979)
1470Å Irradiation of 13.4mb CH_4/NH_3 + 666mb H_2 (Raulin et al., 1979)
Titan, Normal Hydrocarbons
Titan, Acetylenes
Black Sea Hydrocarbon Sediments, 50m Depth (suspected abiogenic) (Hunt & Whelan, 1978)
Nonesuch Shale Hydrocarbons (Hunt, 1979)
17MeV e^- Irradiation of 950mb CH_4/N_2 (Balestic, 1974)
1236Å Irradiation of 2.6mb CH_4 (Chang, et al., 1979)
Photochemical Model : Column Abundance of Polyacetylenes (Allen et al., 1980)
Black Sea Hydrocarbon Sediments, 1 km Depth (suspected abiogenic) (Hunt & Whelan, 1978)
α=0.25
α=0.5
α=1.0

Figure 2

Figure 3

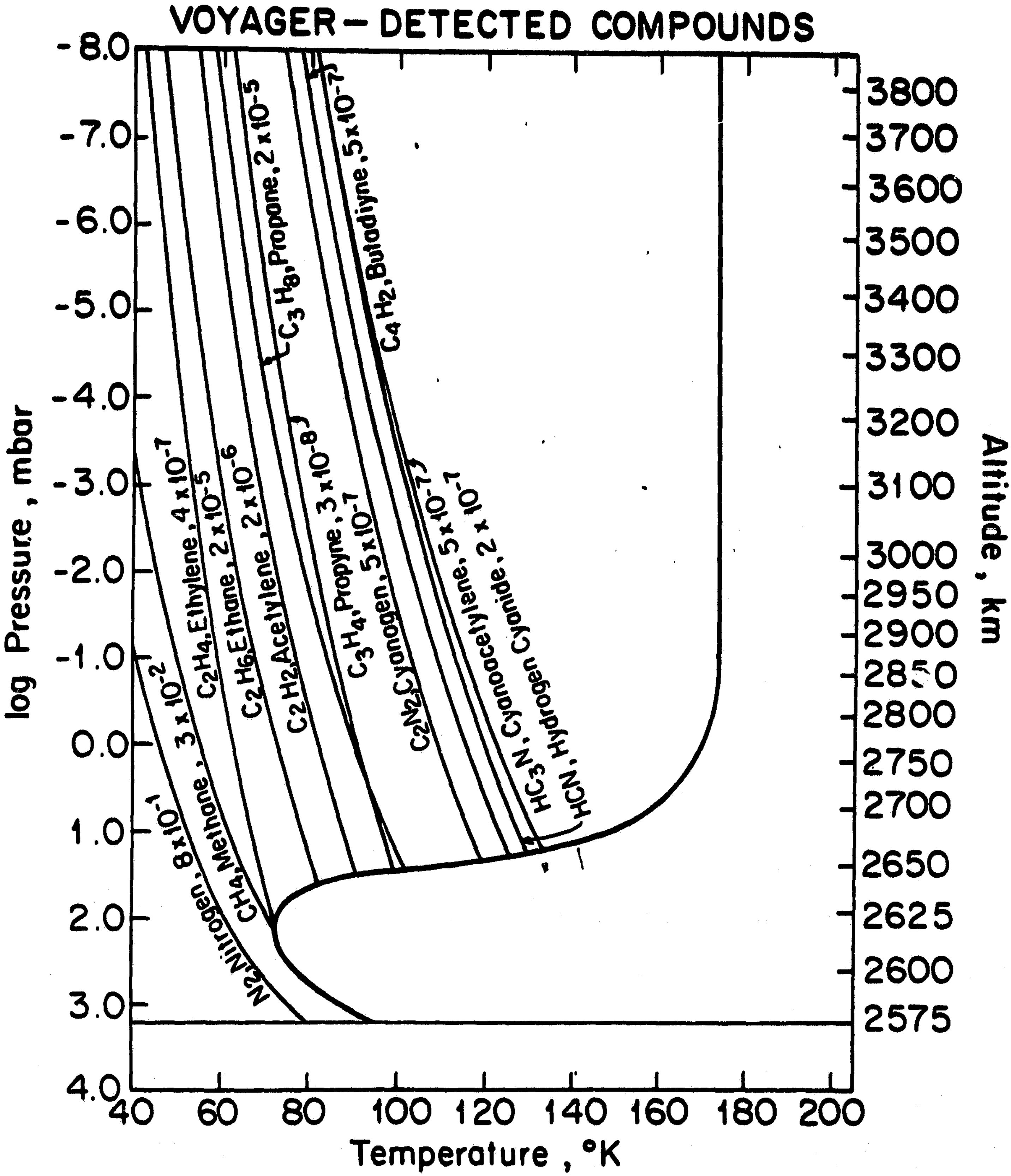
VOYAGER – DETECTED COMPOUNDS
log Pressure, mbar
-8.0
-7.0
-6.0
-5.0
-4.0
-3.0
-2.0
-1.0
0.0
1.0
2.0
3.0
4.0
Altitude, km
3800
3700
3600
3500
3400
3300
3200
3100
3000
2950
2900
2850
2800
2750
2700
2650
2625
2600
2575
Temperature, °K
40
60
80
100
120
140
160
180
200
N_2, Nitrogen, 8×10^{-1}
CH_4, Methane, 3×10^{-2}
C_2H_4, Ethylene, 4×10^{-7}
C_2H_6, Ethane, 2×10^{-5}
C_2H_2, Acetylene, 2×10^{-6}
C_3H_8, Propane, 2×10^{-5}
C_3H_4, Propyne, 3×10^{-8}
C_2N_2, Cyanogen, 5×10^{-7}
C_4H_2, Butadiyne, 5×10^{-7}
HC_3N, Cyanoacetylene, 5×10^{-7}
HCN, Hydrogen Cyanide, 2×10^{-7}

Figure 4a

ALIPHATIC HYDROCARBON SERIES

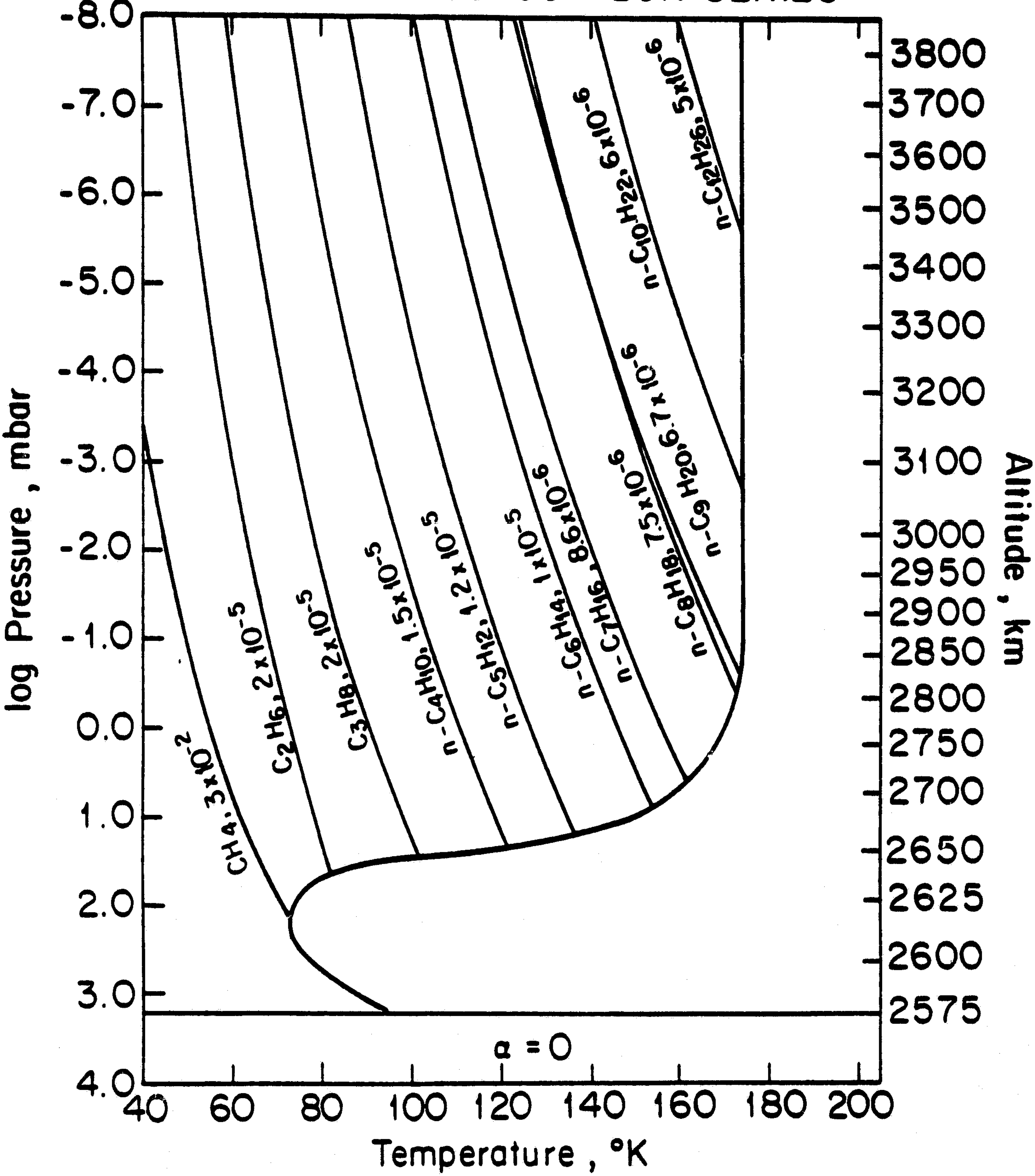

ORIGINAL PAGE IS
OF POOR QUALITY

Figure 4b

ALIPHATIC HYDROCARBON SERIES

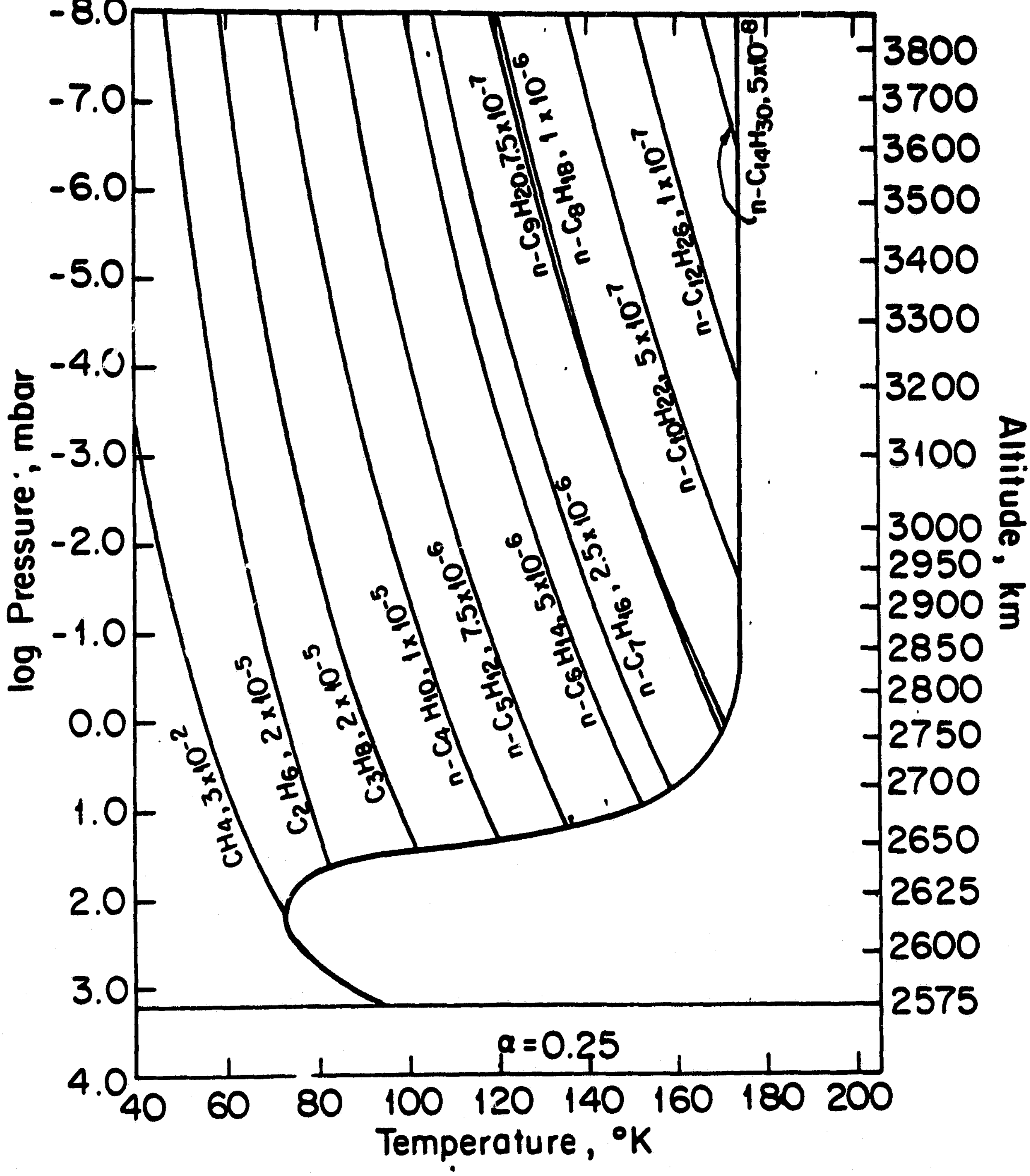

Figure 4c

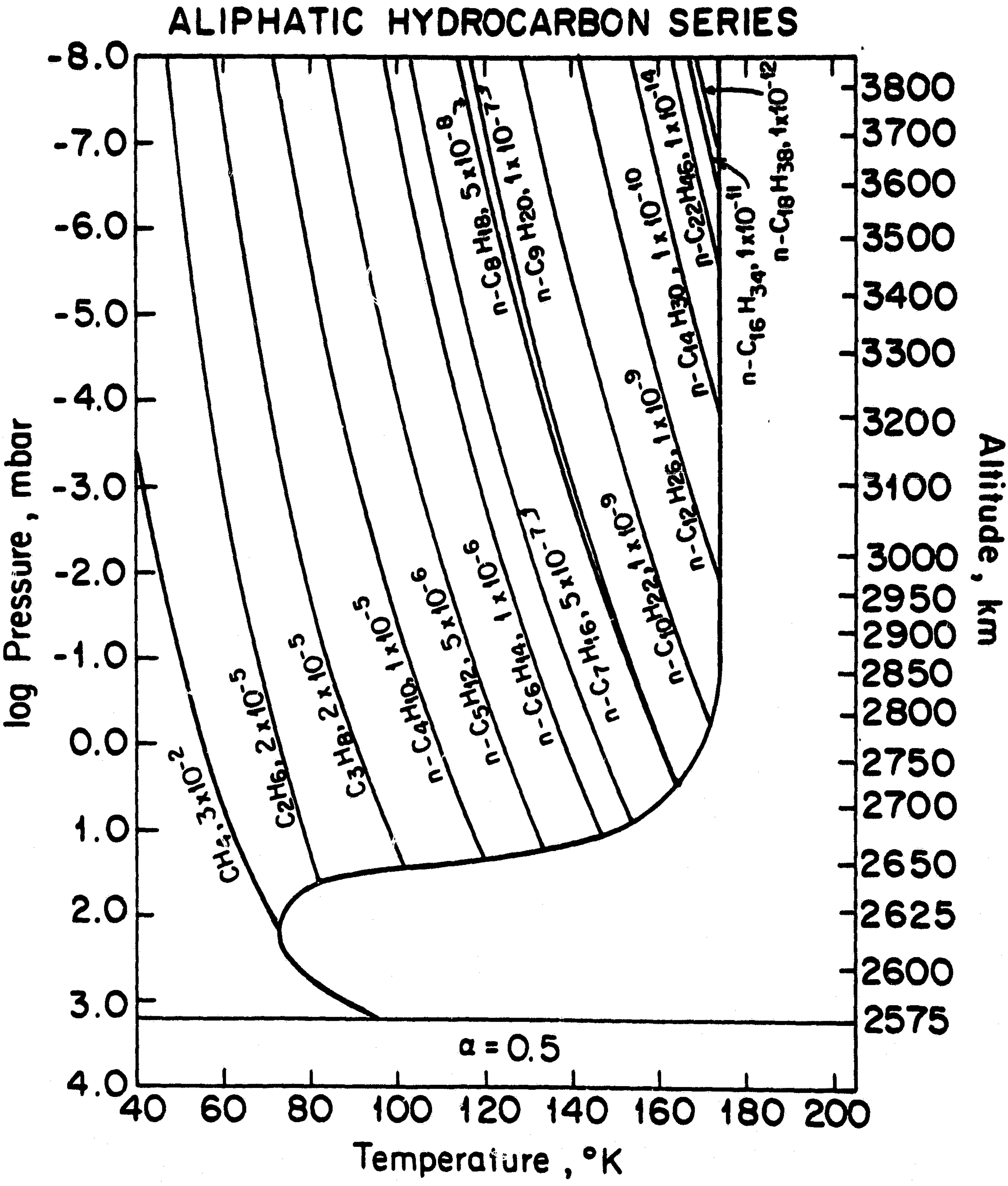
ALIPHATIC HYDROCARBON SERIES
log Pressure , mbar
-8.0
-7.0
-6.0
-5.0
-4.0
-3.0
-2.0
-1.0
0.0
1.0
2.0
3.0
4.0
Temperature , °K
40
60
80
100
120
140
160
180
200
Altitude , km
3800
3700
3600
3500
3400
3300
3200
3100
3000
2950
2900
2850
2800
2750
2700
2650
2625
2600
2575
CH_4, 3×10^{-2}
C_2H_6, 2×10^{-5}
C_3H_8, 2×10^{-5}
n-C_4H_{10}, 1×10^{-5}
n-C_5H_{12}, 5×10^{-6}
n-C_6H_{14}, 1×10^{-6}
n-C_7H_{16}, 5×10^{-7}
n-C_8H_{18}, 5×10^{-8}
n-C_9H_{20}, 1×10^{-7}
n-$C_{10}H_{22}$, 1×10^{-9}
n-$C_{12}H_{26}$, 1×10^{-9}
n-$C_{14}H_{30}$, 1×10^{-10}
n-$C_{16}H_{34}$, 1×10^{-11}
n-$C_{18}H_{38}$, 1×10^{-12}
n-$C_{22}H_{46}$, 1×10^{-14}
$\alpha = 0.5$

ORIGINAL PAGE IS OF POOR QUALITY

Figure 4d

ALIPHATIC HYDROCARBON SERIES

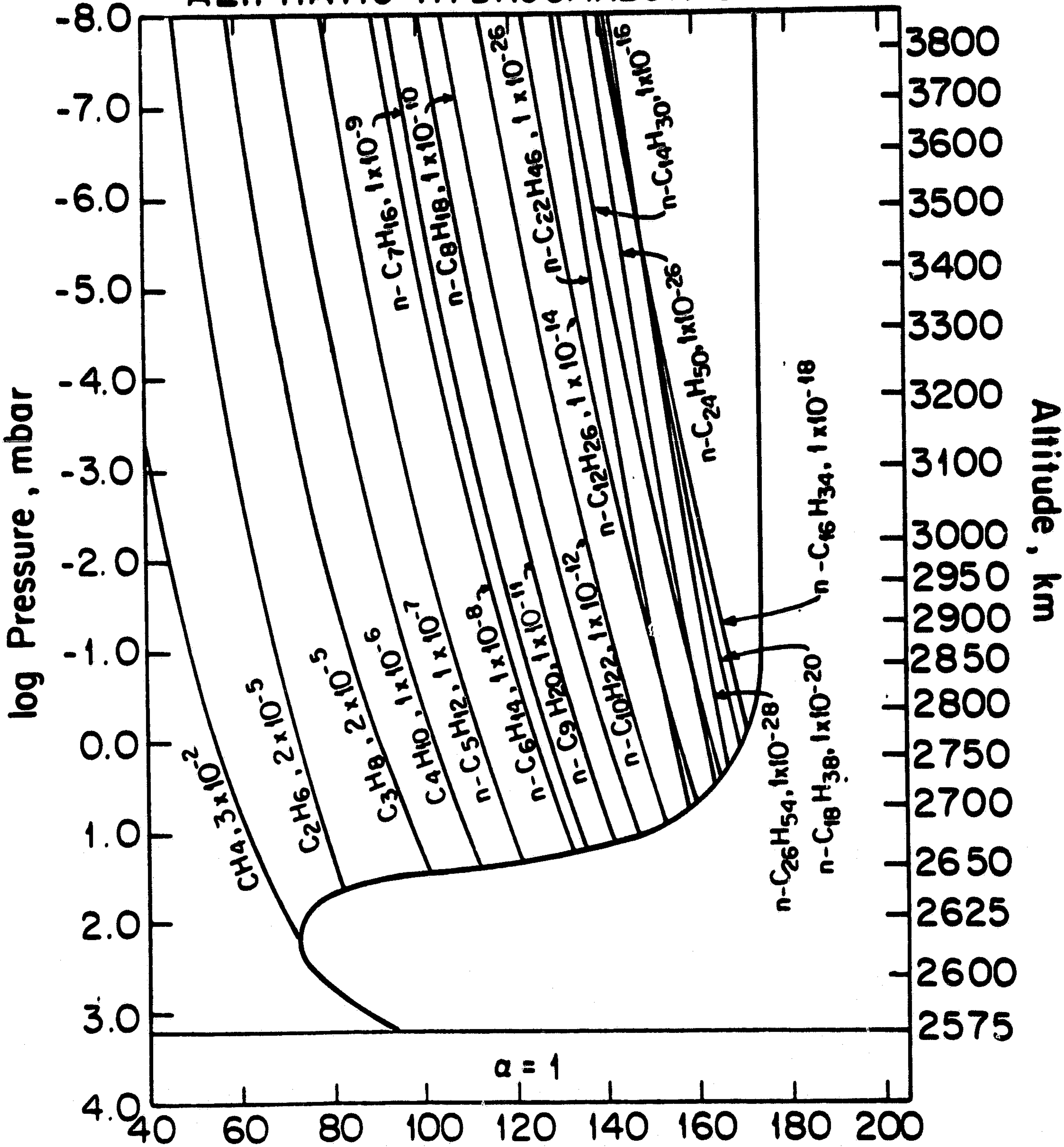

ORIGINAL PAGE IS
OF POOR QUALITY

Figure 5a

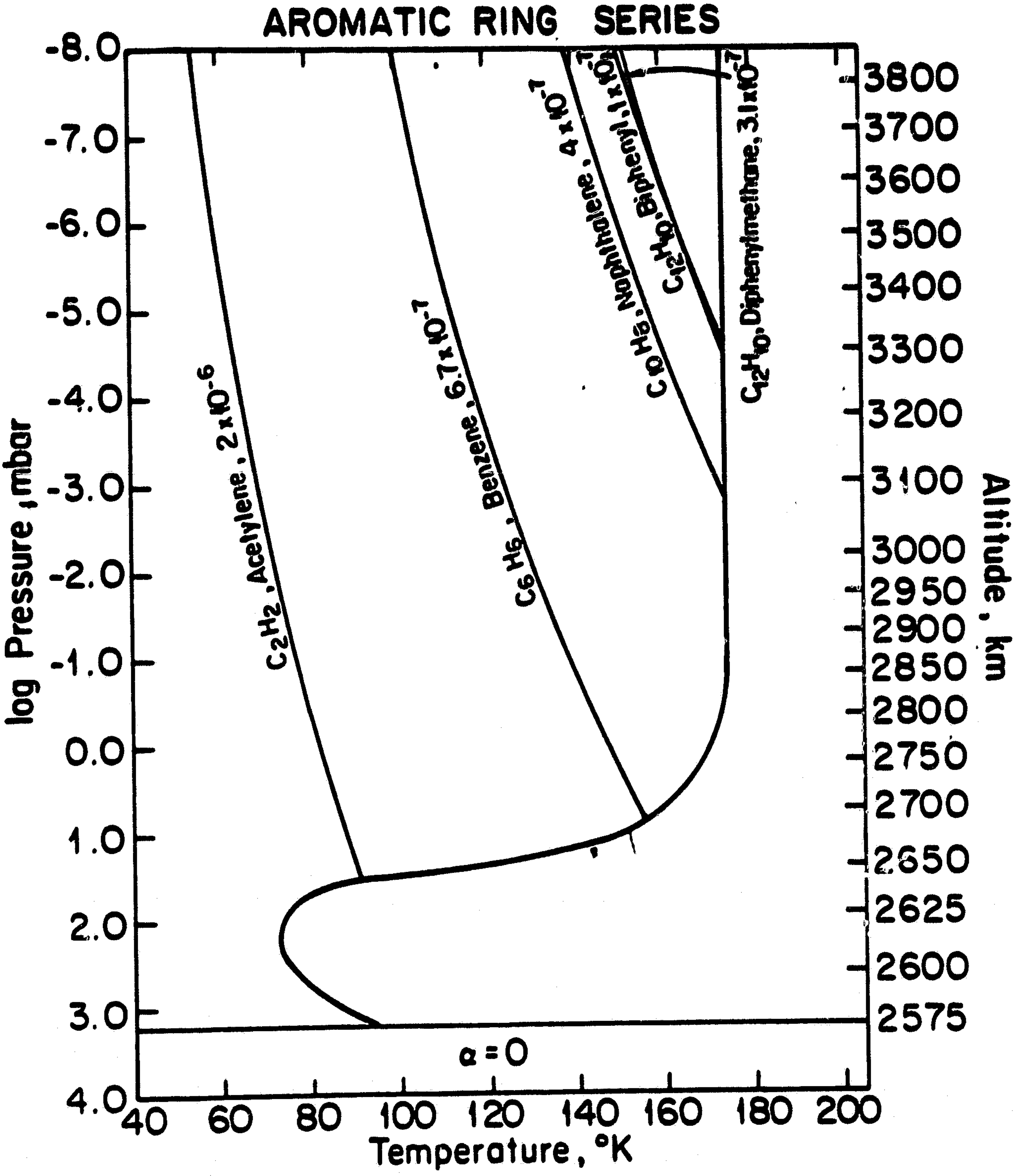

Figure 5b

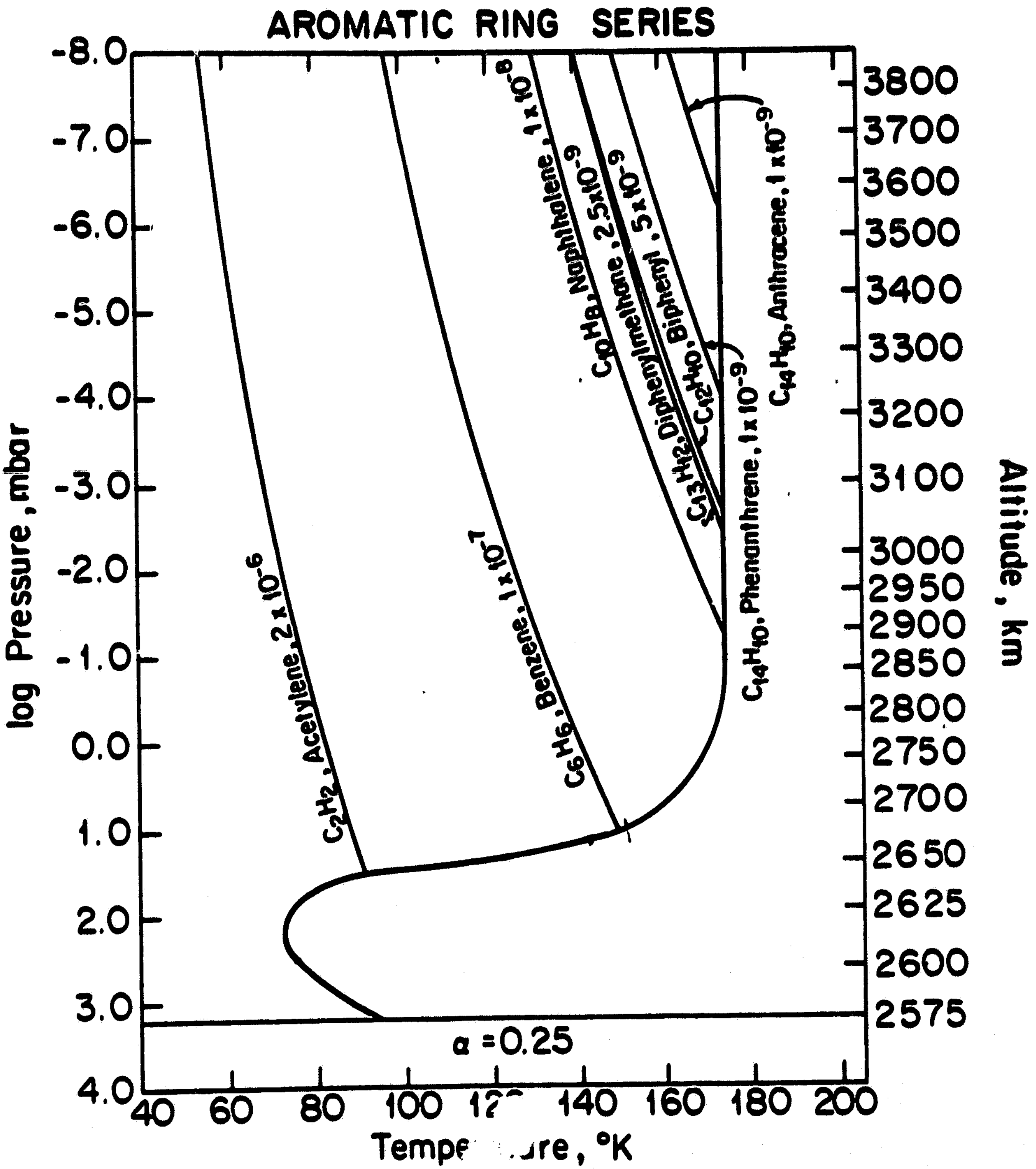
AROMATIC RING SERIES
log Pressure, mbar
-8.0
-7.0
-6.0
-5.0
-4.0
-3.0
-2.0
-1.0
0.0
1.0
2.0
3.0
4.0
Altitude, km
3800
3700
3600
3500
3400
3300
3200
3100
3000
2950
2900
2850
2800
2750
2700
2650
2625
2600
2575
Temperature, °K
40
60
80
100
120
140
160
180
200
C2H2, Acetylene, 2 x 10^-6
C6H6, Benzene, 1 x 10^-7
C10H8, Naphthalene, 1 x 10^-8
C13H12, Diphenylmethane, 2.5x10^-9
C12H10, Biphenyl, 5 x 10^-9
C14H10, Phenanthrene, 1 x 10^-9
C14H10, Anthracene, 1 x 10^-9
α = 0.25

ORIGINAL PAGE IS
OF POOR QUALITY

Figure 5c

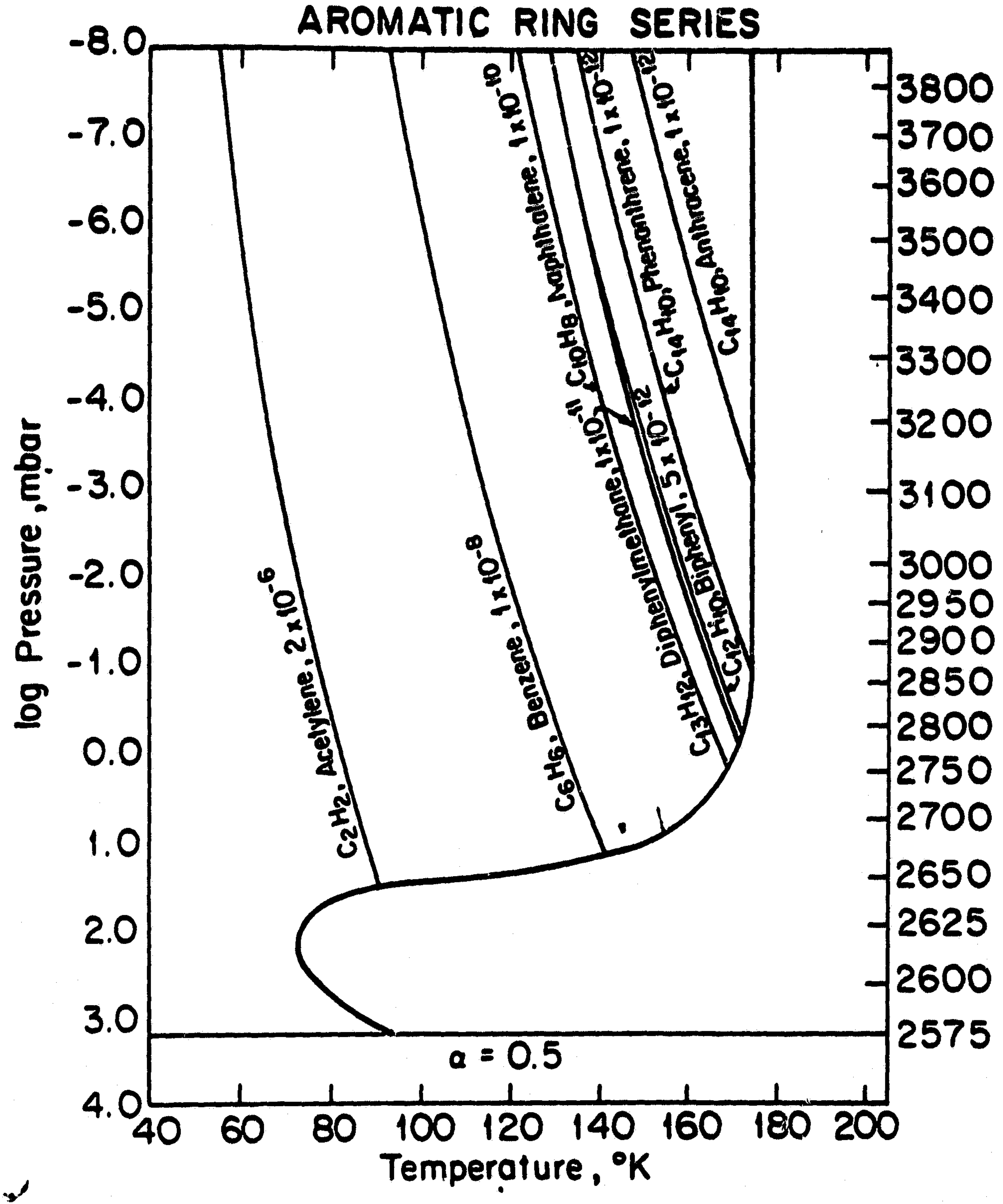

Figure 5d

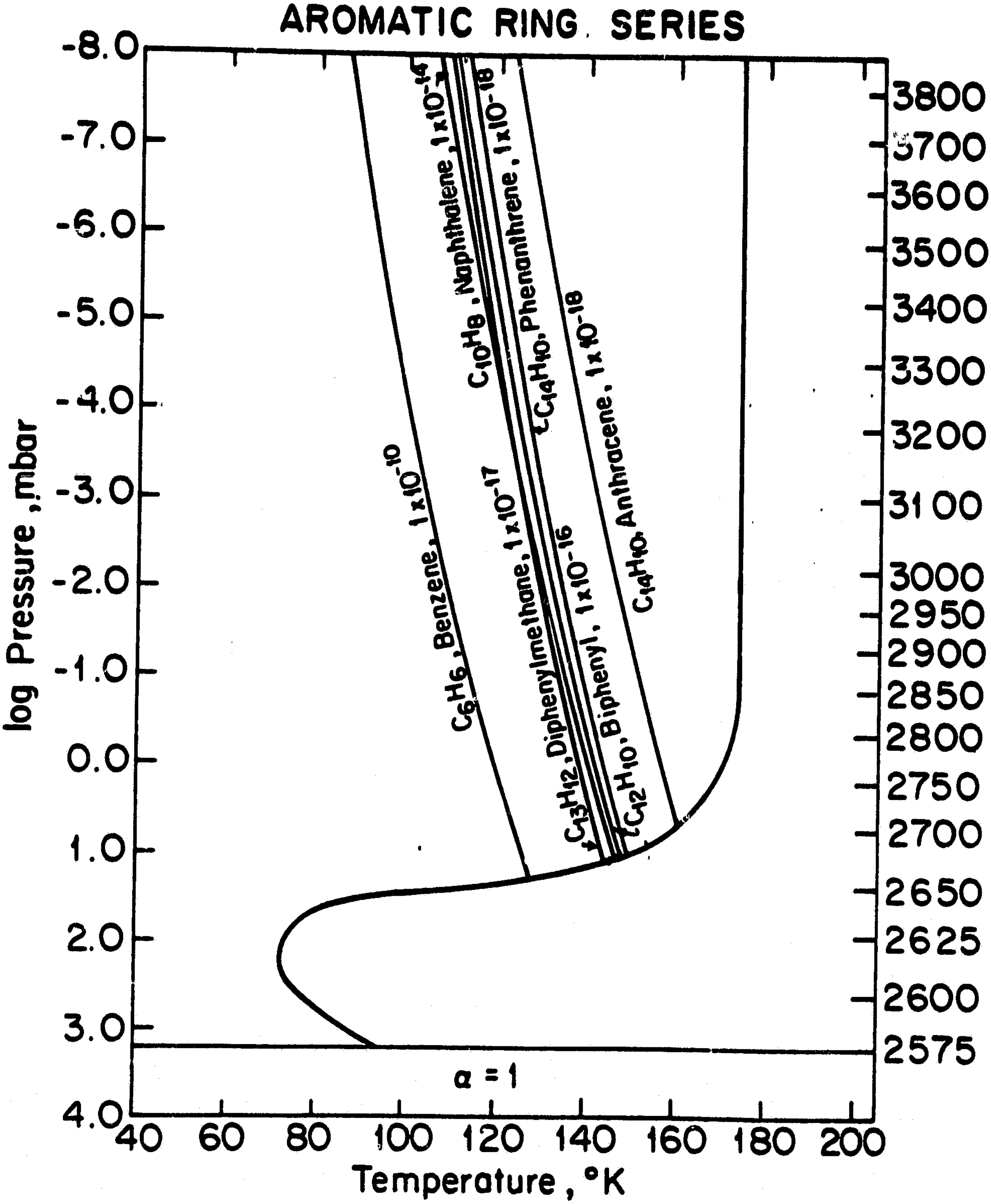
AROMATIC RING SERIES
log Pressure, mbar
-8.0
-7.0
-6.0
-5.0
-4.0
-3.0
-2.0
-1.0
0.0
1.0
2.0
3.0
4.0
Temperature, °K
40
60
80
100
120
140
160
180
200
Altitude, km
3800
3700
3600
3500
3400
3300
3200
3100
3000
2950
2900
2850
2800
2750
2700
2650
2625
2600
2575
C_6H_6, Benzene, 1×10^{-10}
$C_{10}H_8$, Naphthalene, 1×10^{-14}
$C_{14}H_{10}$, Phenanthrene, 1×10^{-18}
$C_{14}H_{10}$, Anthracene, 1×10^{-18}
$C_{13}H_{12}$, Diphenylmethane, 1×10^{-17}
$C_{12}H_{10}$, Biphenyl, 1×10^{-16}
$\alpha = 1$

Figure 6a

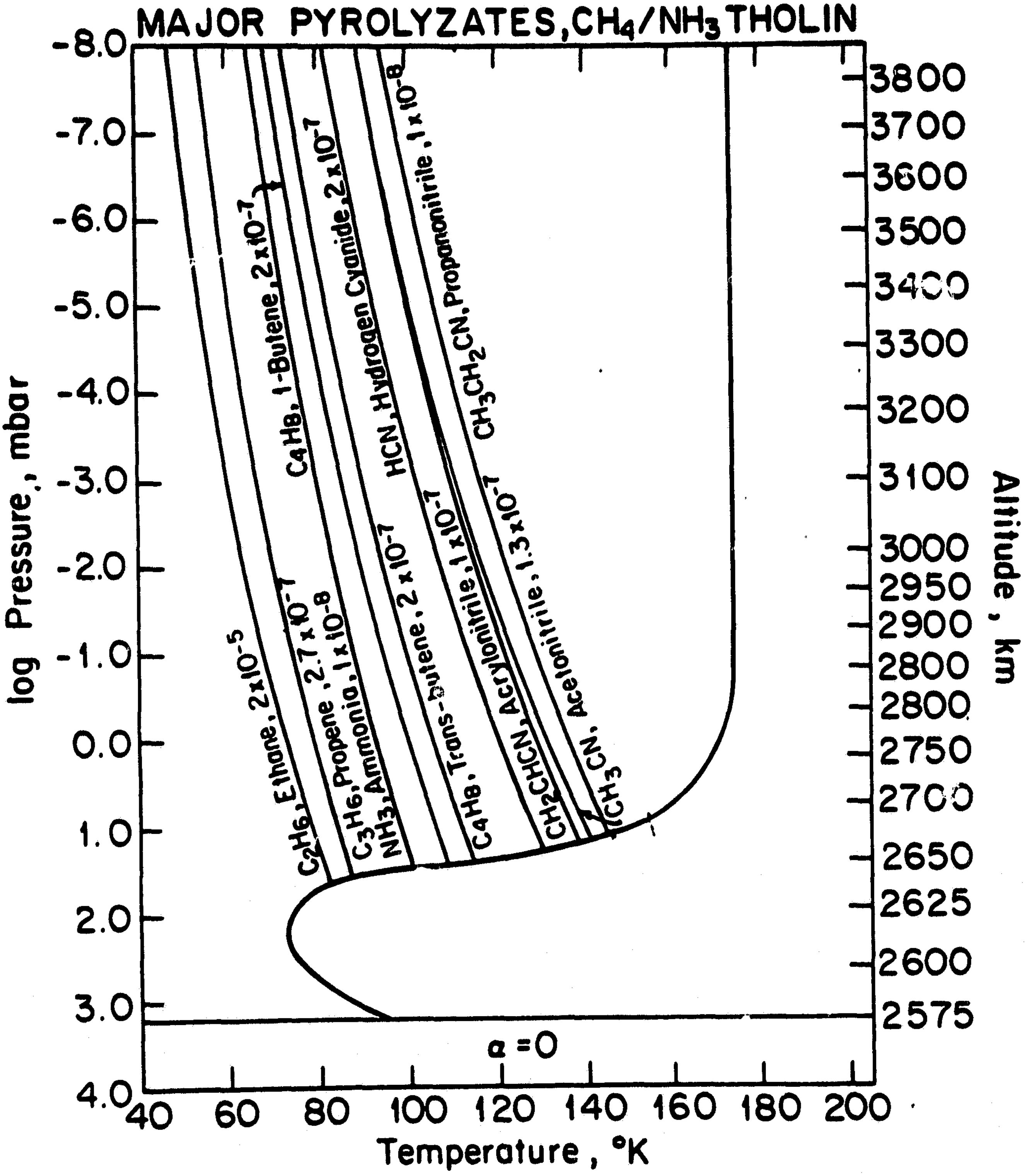
MAJOR PYROLYZATES, CH4/NH3 THOLIN
log Pressure, mbar
-8.0
-7.0
-6.0
-5.0
-4.0
-3.0
-2.0
-1.0
0.0
1.0
2.0
3.0
4.0
Altitude, km
3800
3700
3600
3500
3400
3300
3200
3100
3000
2950
2900
2800
2800
2750
2700
2650
2625
2600
2575
Temperature, °K
40
60
80
100
120
140
160
180
200
C2H6, Ethane, 2x10-5
C3H6, Propene, 2.7x10-7
NH3, Ammonia, 1x10-8
C4H8, 1-Butene, 2x10-7
HCN, Hydrogen Cyanide, 2x10-7
C4H8, Trans-butene, 2x10-7
CH2CHCN, Acrylonitrile, 1x10-7
CH3CN, Acetonitrile, 1.3x10-7
CH3CH2CN, Propanonitrile, 1x10-8
α = 0

Figure 6b

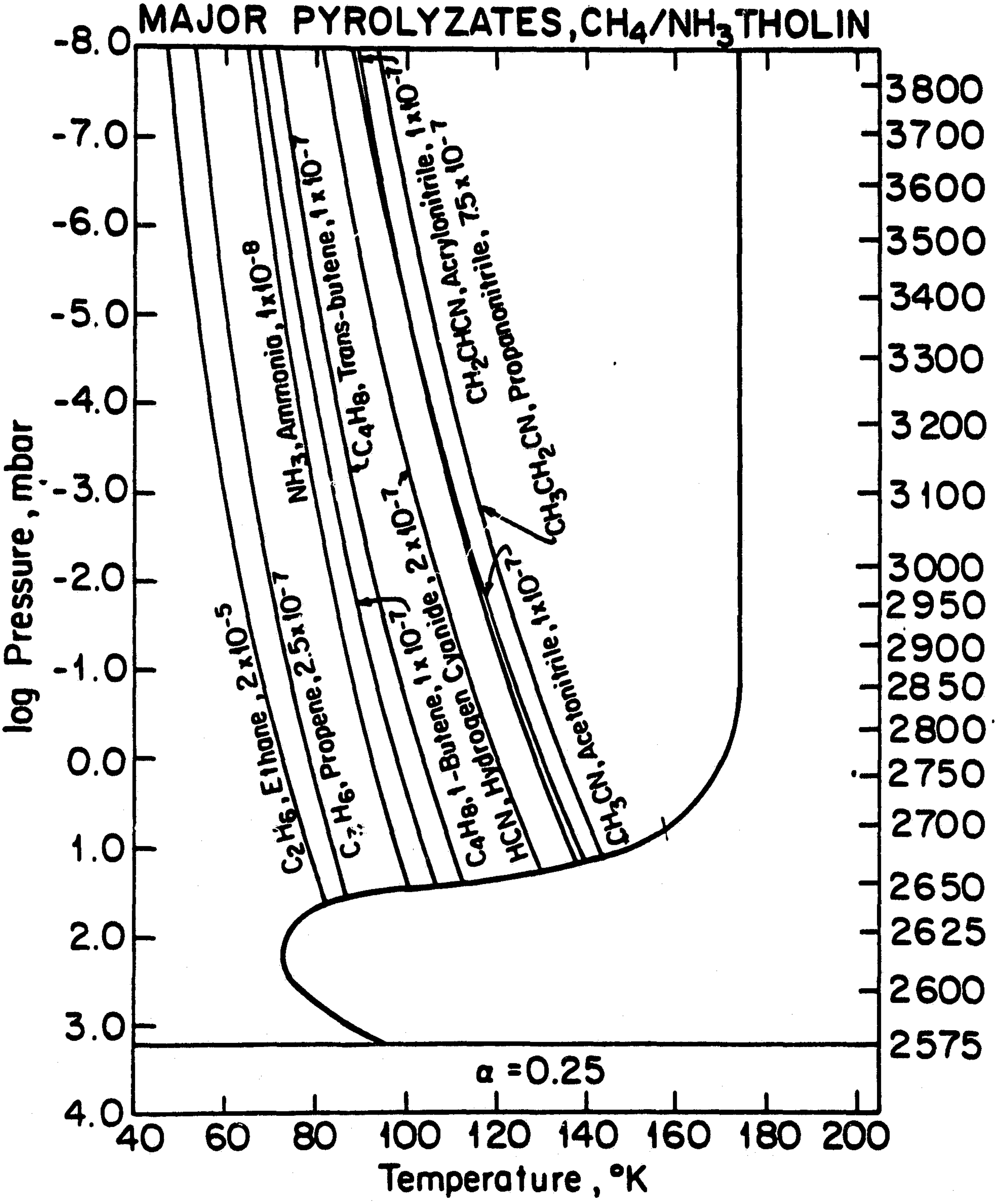
MAJOR PYROLYZATES, CH_4/NH_3 THOLIN
log Pressure, mbar
-8.0
-7.0
-6.0
-5.0
-4.0
-3.0
-2.0
-1.0
0.0
1.0
2.0
3.0
4.0
Temperature, °K
40
60
80
100
120
140
160
180
200
Altitude, km
3800
3700
3600
3500
3400
3300
3200
3100
3000
2950
2900
2850
2800
2750
2700
2650
2625
2600
2575
C_2H_6, Ethane, 2×10^{-5}
C_3H_6, Propene, 2.5×10^{-7}
NH_3, Ammonia, 1×10^{-8}
C_4H_8, Trans-butene, 1×10^{-7}
C_4H_8, 1-Butene, 1×10^{-7}
HCN, Hydrogen Cyanide, 2×10^{-7}
CH_2CHCN, Acrylonitrile, 1×10^{-7}
CH_3CH_2CN, Propanonitrile, 7.5×10^{-7}
CH_3CN, Acetonitrile, 1×10^{-7}
$\alpha = 0.25$

Figure 6c

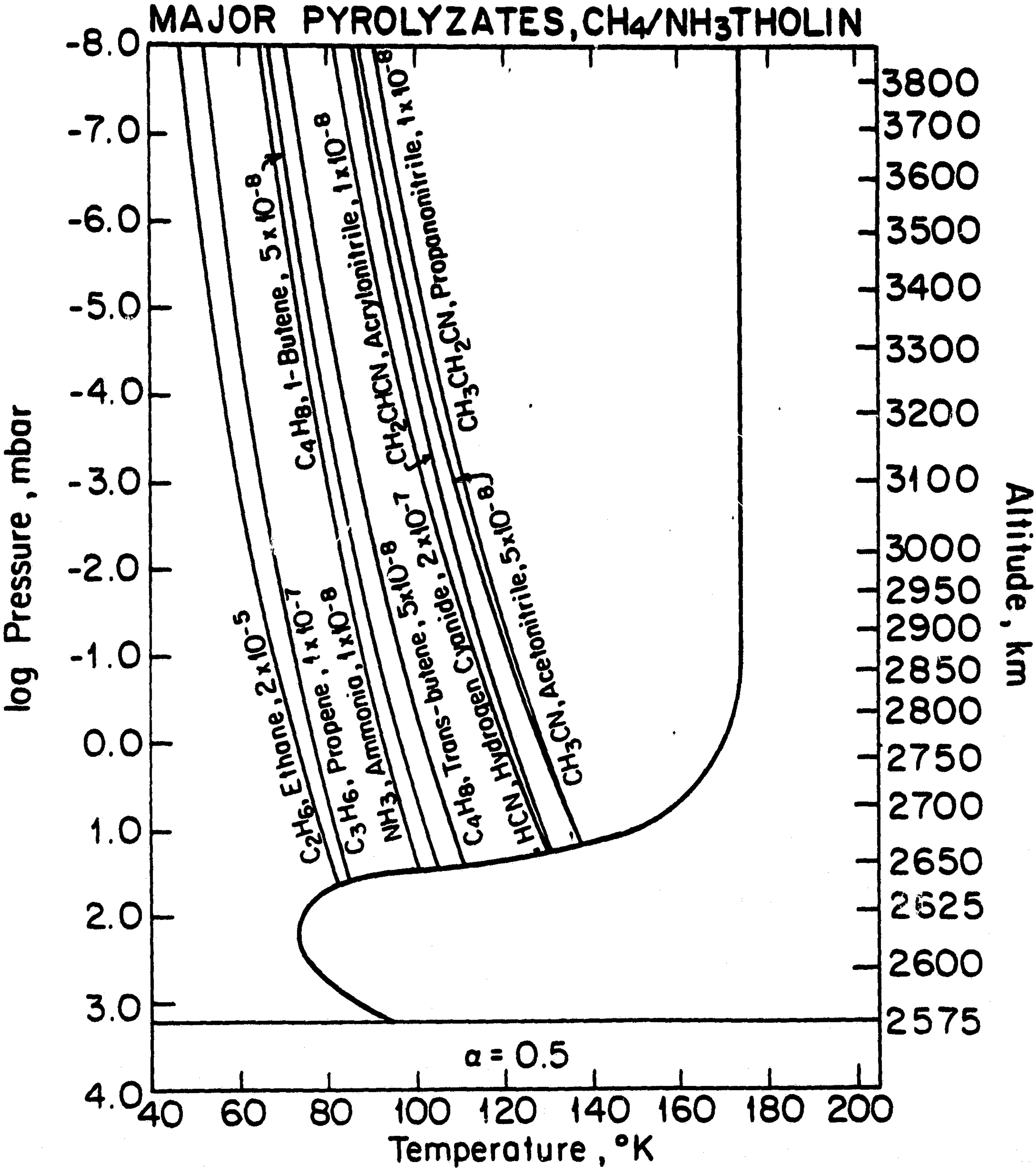
MAJOR PYROLYZATES, CH_4/NH_3 THOLIN
log Pressure, mbar
-8.0
-7.0
-6.0
-5.0
-4.0
-3.0
-2.0
-1.0
0.0
1.0
2.0
3.0
4.0
Altitude, km
3800
3700
3600
3500
3400
3300
3200
3100
3000
2950
2900
2850
2800
2750
2700
2650
2625
2600
2575
Temperature, °K
40
60
80
100
120
140
160
180
200
C_4H_8, 1-Butene, 5×10^{-8}
CH_2CHCN, Acrylonitrile, 1×10^{-8}
CH_3CH_2CN, Propanonitrile, 1×10^{-8}
C_2H_6, Ethane, 2×10^{-5}
C_3H_6, Propene, 1×10^{-7}
NH_3, Ammonia, 1×10^{-8}
C_4H_8, Trans-butene, 5×10^{-8}
HCN, Hydrogen Cyanide, 2×10^{-7}
CH_3CN, Acetonitrile, 5×10^{-8}
$\alpha = 0.5$

Figure 6d

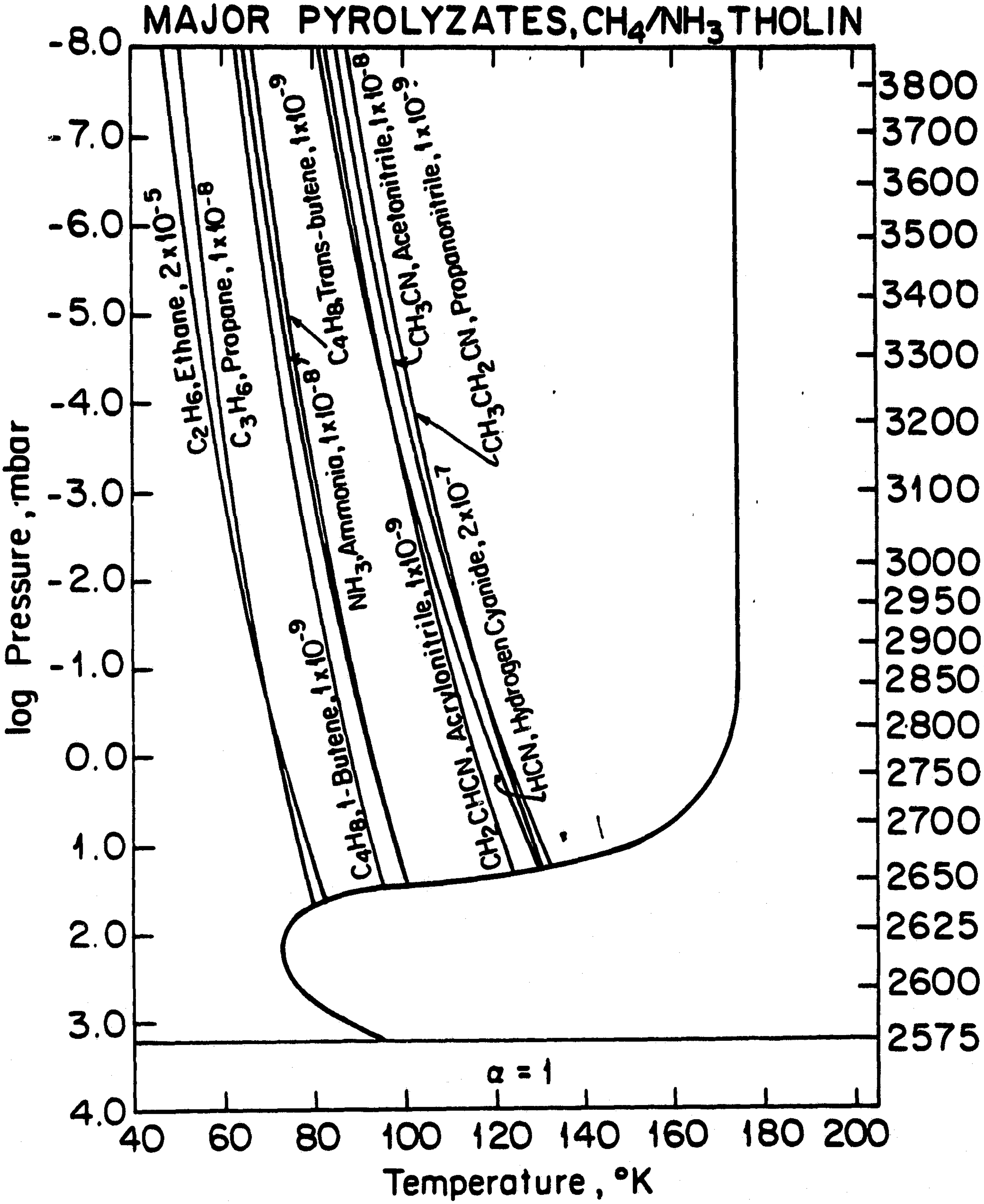
MAJOR PYROLYZATES, CH_4/NH_3 THOLIN
log Pressure, mbar
-8.0
-7.0
-6.0
-5.0
-4.0
-3.0
-2.0
-1.0
0.0
1.0
2.0
3.0
4.0
Temperature, °K
40
60
80
100
120
140
160
180
200
Altitude, km
3800
3700
3600
3500
3400
3300
3200
3100
3000
2950
2900
2850
2800
2750
2700
2650
2625
2600
2575
C_2H_6, Ethane, 2×10^{-5}
C_3H_8, Propane, 1×10^{-8}
C_4H_8, Trans-butene, 1×10^{-9}
NH_3, Ammonia, 1×10^{-8}
CH_3CN, Acetonitrile, 1×10^{-8}
CH_3CH_2CN, Propanonitrile, 1×10^{-9}
C_4H_8, 1-Butene, 1×10^{-9}
CH_2CHCN, Acrylonitrile, 1×10^{-9}
HCN, Hydrogen Cyanide, 2×10^{-7}
$\alpha = 1$

Figure 7a

MINOR PYROLYZATES, CH_4/NH_3 THOLIN

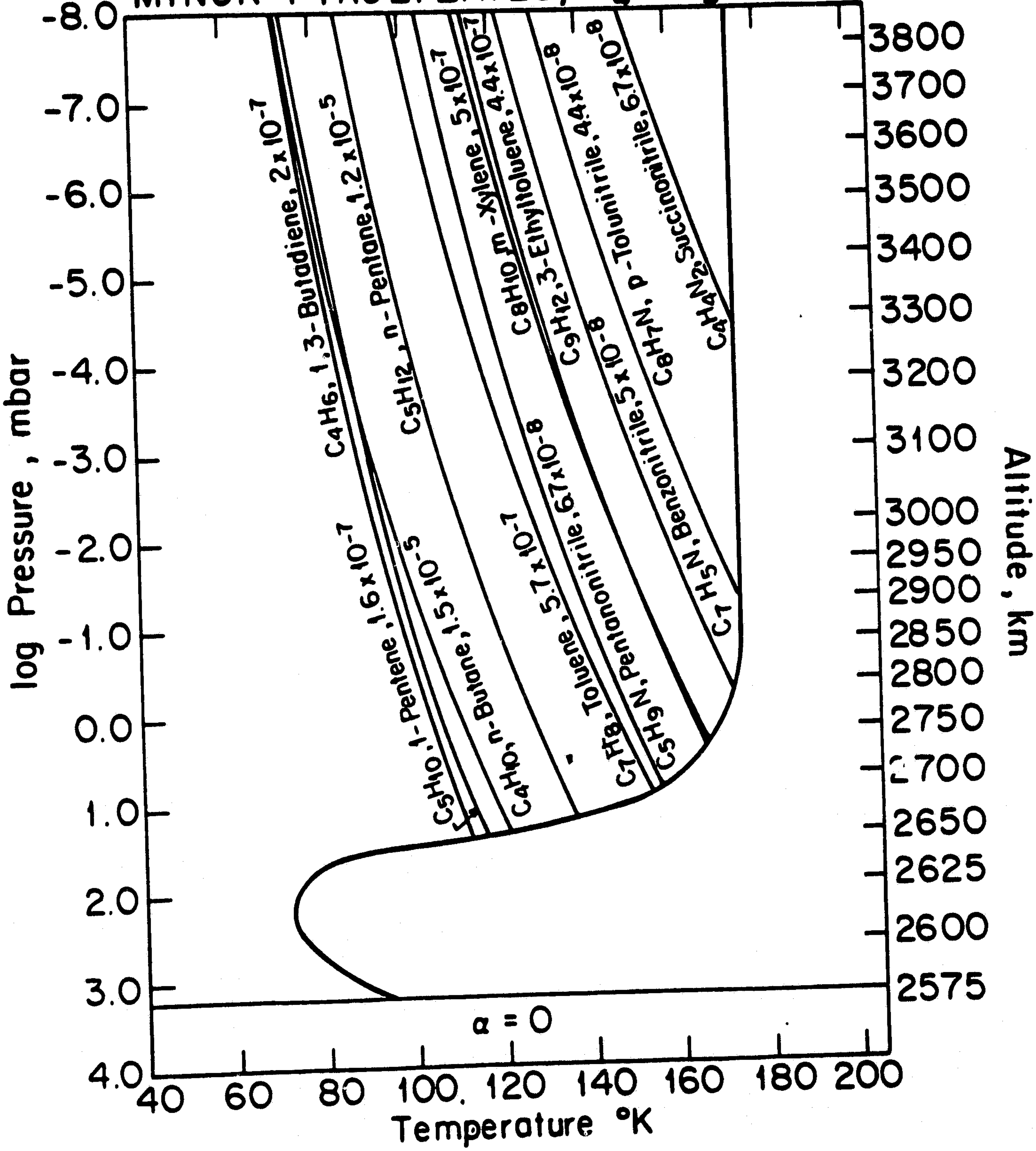

Figure 7b

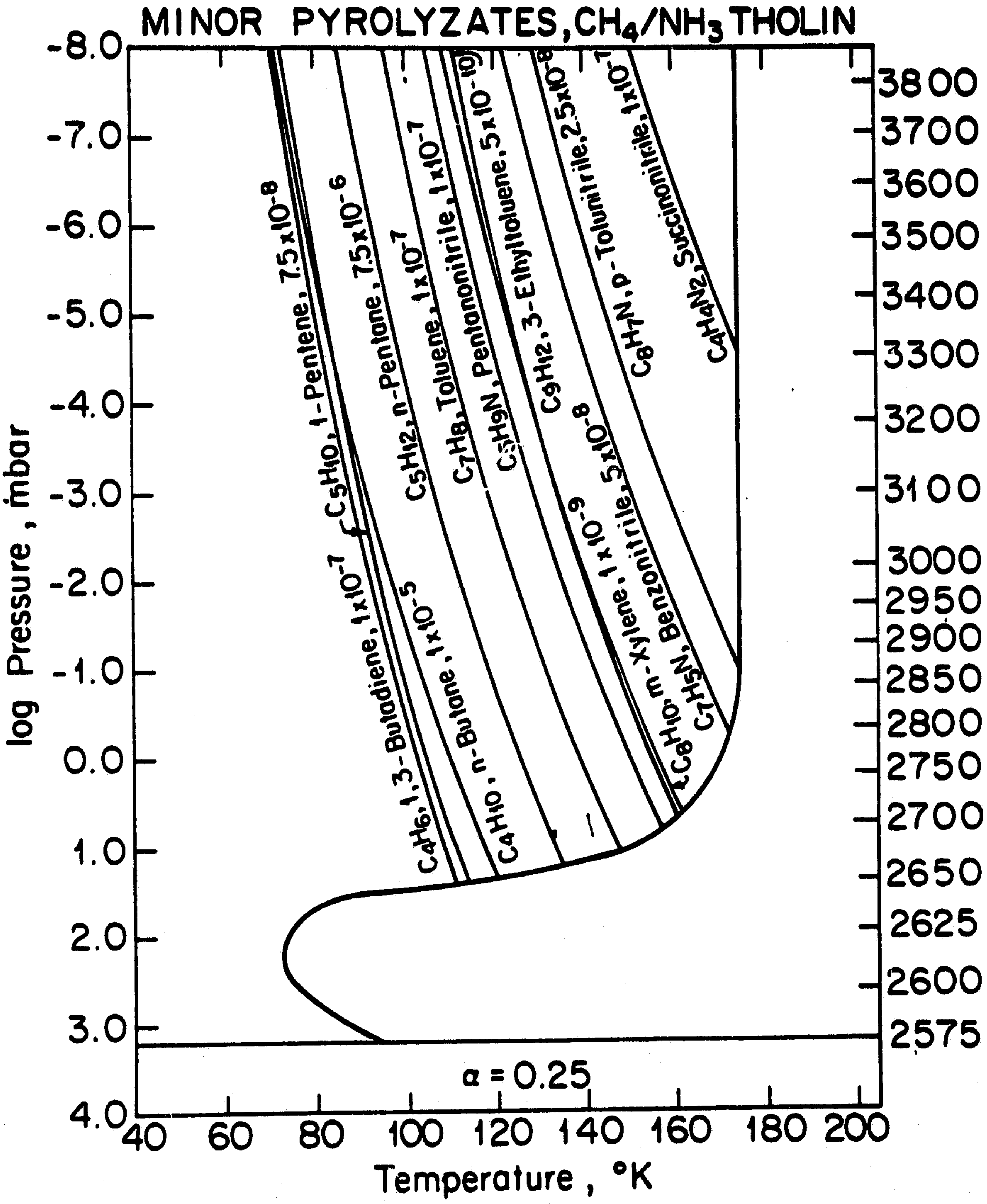
MINOR PYROLYZATES, CH_4/NH_3 THOLIN
log Pressure, mbar
-8.0
-7.0
-6.0
-5.0
-4.0
-3.0
-2.0
-1.0
0.0
1.0
2.0
3.0
4.0
Temperature, °K
40
60
80
100
120
140
160
180
200
Altitude, km
3800
3700
3600
3500
3400
3300
3200
3100
3000
2950
2900
2850
2800
2750
2700
2650
2625
2600
2575
α = 0.25
C_4H_6, 1,3-Butadiene, 1x10^{-7}
C_5H_{10}, 1-Pentene, 7.5x10^{-8}
C_4H_{10}, n-Butane, 1x10^{-5}
C_5H_{12}, n-Pentane, 7.5x10^{-6}
C_7H_8, Toluene, 1x10^{-7}
C_5H_9N, Pentanonitrile, 1x10^{-7}
C_9H_{12}, 3-Ethyltoluene, 5x10^{-10}
C_8H_{10}, m-Xylene, 1x10^{-9}
C_7H_5N, Benzonitrile, 5x10^{-8}
C_8H_7N, p-Tolunitrile, 2.5x10^{-8}
$C_4H_4N_2$, Succinonitrile, 1x10^{-7}

Figure 7c

MINOR PYROLYZATES, CH_4/NH_3 THOLIN

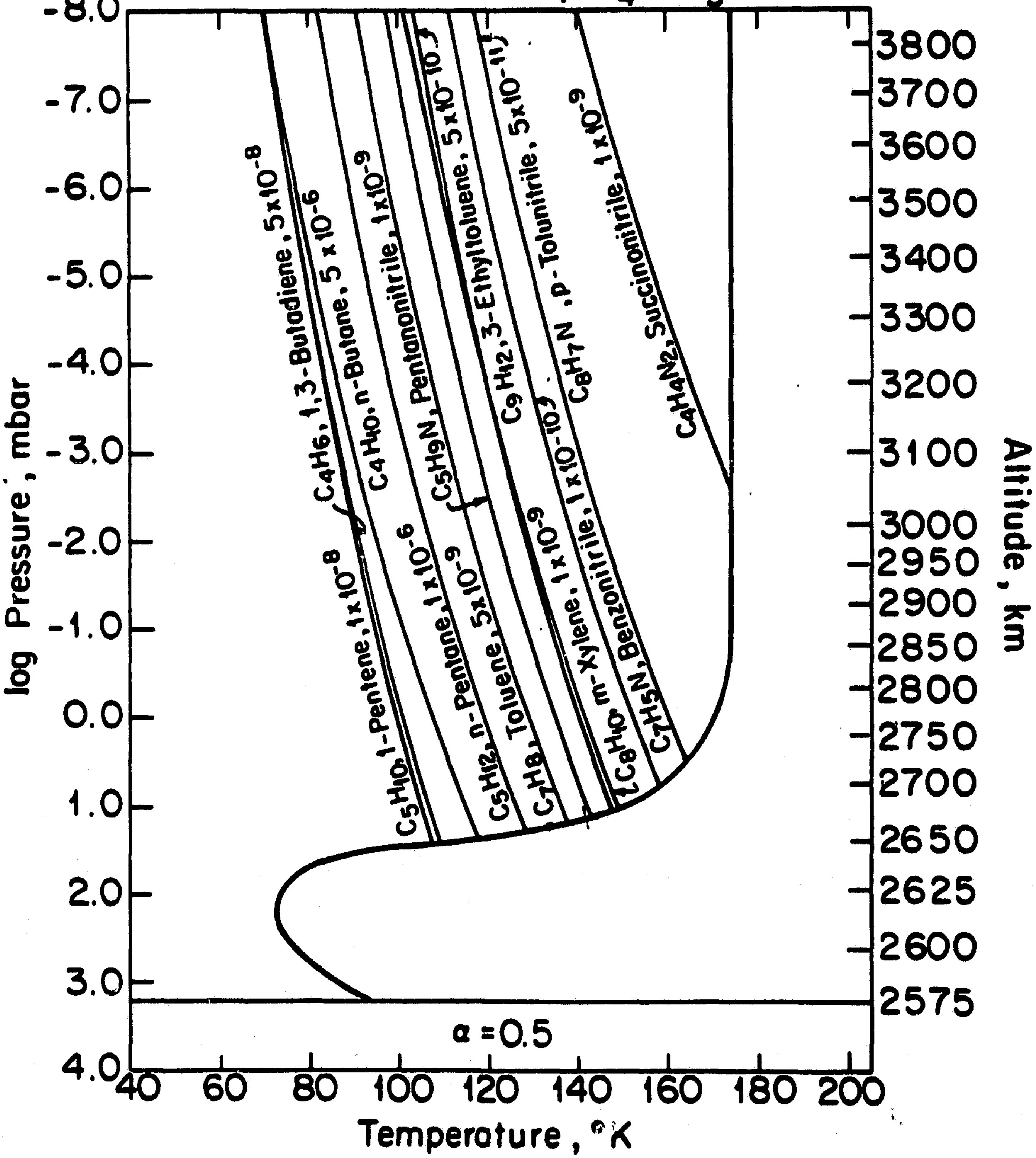

ORIGINAL PAGE IS
OF POOR QUALITY

Figure 7d

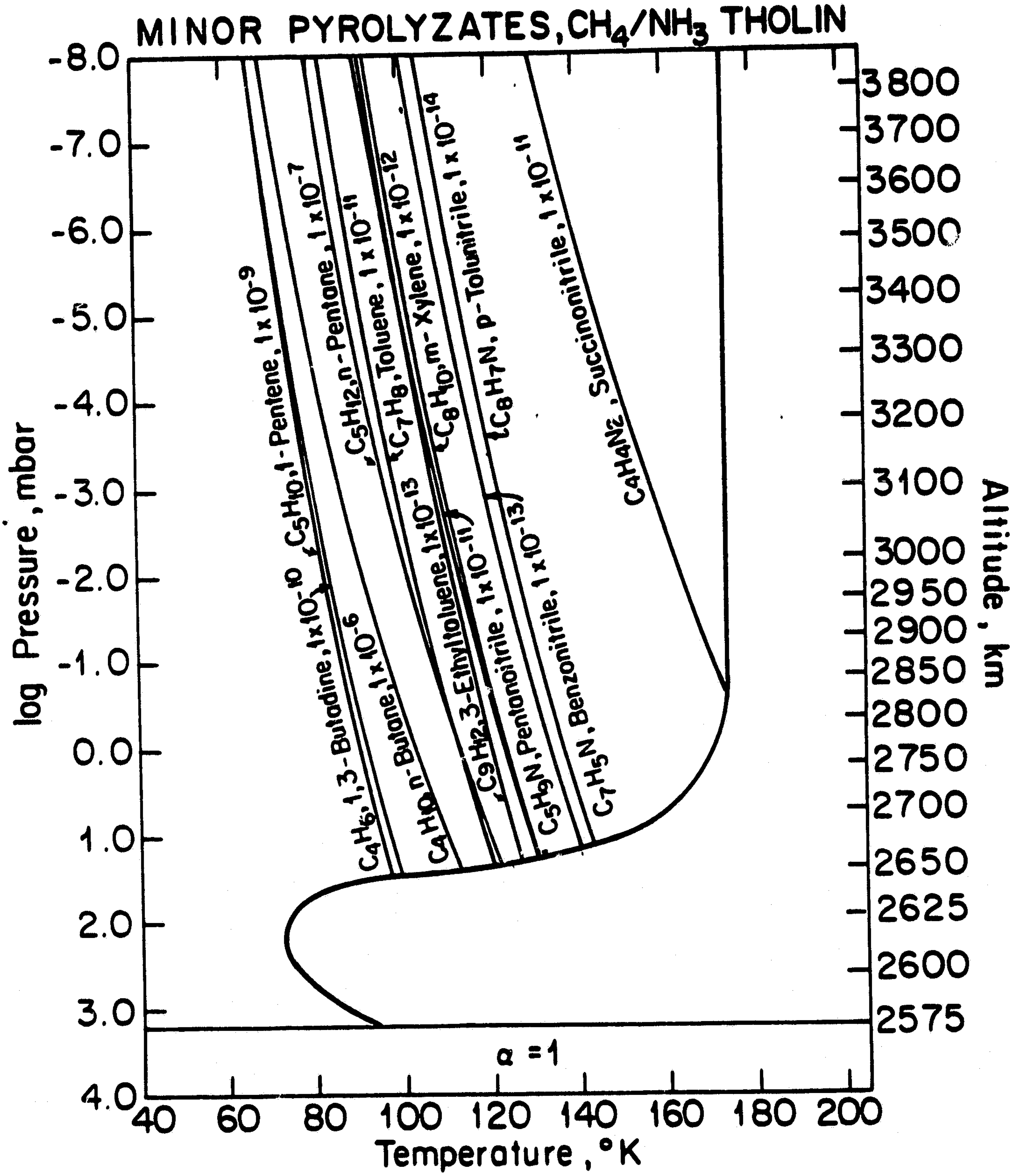

REFERENCES

Allen, C.W. (1965). The interpretation of the XUV solar spectrum. Space Sci. Revs. 4, 91-122.

Allen, M., Pinto, J.P., and Yung, Y.L. (1980). Titan: Aerosol photochemistry and variations related to the sunspot cycle. Astrophys. J. 242, L125-L128.

Axel, L. (1972). Inhomogenous models of the atmosphere of Jupiter. Astrophys. J. 173, 451-468.

Balestic, F.S. (1974). Synthese abiotique d'acides amines par voie radiochimique. Doctoral thesis, University of Paris.

Bar-Nun, A., and Podolak, M. (1974). The photochemistry of hydrocarbons in Titan's atmosphere. Icarus 38, 115-122.

Biswas, S., and Durgaprasad, N. (1980). Skylab measurements of low energy cosmic rays. Space Sci. Revs. 25, 285-327.

Bridge, H.S., Belcher, J.W., Lazarus, A.J., Olbert, S., Sullivan, J.D., Bagenal, F., Gazis, P.R., Hartle, R.E., Ogilvie, K.W., Scudder, J.D., Sittler, E.C., Eviatar, A., Siscoe, G.L., Goertz, C.K., and Vasyliunas, V.M. (1981). Plasma observations near Saturn: Initial results from Voyager 1. Science 212, 217- 224.

Bridge, H.S., Bagenal, F., Belcher, J.W., Lazarus, A.J., McNutt, R.L., Sullivan, J.D., Gazis, P.R., Hartle, R.E. Ogilvie, K.W., Scudder, J.D., Sittler, E.C., Eviatar, A., Siscoe, G.L., Goertz, C.K., and Vasyliunas, V.M. (1982). Plasma observations near Saturn: Initial results from Voyager 2. Science 215, 563-570.

Bridge, H.S. (1981). Private communication.

Broadfoot, A.L., Sandel, B.R., Shemansky, D.E., Holberg, J.B., Smith, G.R., Strobel, D.F., McConnell, J.C., Kumar, S., Hunten, D.M., Atreya, S.K., Donahue, T.M., Moos, H.W., Bertaux, J.L., Blamont, J.E., Pomphrey, R.B., and Linick, S. (1981). Extreme ultraviolet observations from Voyager 1 encounter with Saturn. Science 212, 206-211.

Caldwell, J.J. (1974). Ultraviolet observations of Titan from OAO-2. In The Atmosphere of Titan (D. Hunten, Ed.). NASA Special Publication SP-340, Washington, D.C.

Capone, L.A., Prasad, S.S., Huntress, W.T., Whitten, R.C., Dubach, J., and Santhanam, K. (1981). Formation of organic molecules on Titan. Nature 293, 45-46.

Chang, S., Scattergood, T., Aronowitz, S., and Flores, J. (1979). Organic chemistry on Titan. Rev. Geophys. Space Phys. 17, 1923-1933.

Cook, C.J., Jones, E., Jr., and Jorgensen, T., Jr. (1953). Range-energy relations of 10 to 250-keV protons and helium ions in various gases. Phys. Rev. 91, 1417-1422.

Danielson, R.E., Caldwell, J.J., and Larach, D.R. (1974). An inversion in the atmosphere of Titan. In The Atmosphere of Titan (D. Hunten, Ed.). NASA Special Publication SP-340, Washington, D.C.

Friedlander, G., Kennedy, J.W., and Miller, J.M. (1964). Nuclear and Radiochemistry, 2nd Ed. John Wiley, New York.

Gillett, F.C., Forrest, W.J., and Merrill, K.M. (1973). 8-13 μm observations of Titan. Astrophys. J. Letters 184, 93-95.

Gupta, S., Ochiai, E., and Ponnamperuma, C. (1981). Organic synthesis in the atmosphere of Titan. Nature 293, 725-727.

Hanel, R., Conrath, B., Flasar, F.M., Kunde, V., Maguire, W., Pearl, J., Pirraglia, J., Samuelson, R., Herath, L., Allison, M., Cruikshank, D., Gautier, D., Gierasch, P., Horn, L., Koppany, R., and Ponnamperuma, C. (1981). Infrared observations of the Saturnian system from Voyager 1. Science 212, 192-200.

Harris, D.L. (1961). Photometry and colorimetry of planets and satellites. In Planets and Satellites (G.P. Kuiper and B.M. Middlehurst, Eds.), Univ. Chicago Press, Chicago, IL.

Heroux, L., and Hinteregger, H.E. (1978). Aeronomical reference spectrum for solar UV below 2000 angstroms. J. Geophys. Res. 83, 5305-5308.

Hunt, J.M. (1979). Petroleum Geochemistry and Geology. W.H. Freeman, San Francisco, 20.

Hunt, J.M., and Whelan, J.K. (1978). Dissolved gases in Black Sea sediments. In Initial Reports of Deep Drilling Project, Leg 42B 42, part 2, (D.A. Ross and Y.P. Neprochov, Eds.), pp. 661-665. U.S. Government Printing Office, Washington, D.C.

Khare, B.N., Gradie, J., and Sagan, C. (1981). Reflection spectra of simulated Titan organic clouds. *Bull. Amer. Astron. Soc.* *13*, 701.

Khare, B.N., and Sagan, C. (1973). Red clouds in reducing atmospheres. *Icarus* *20*, 311-321.

Khare, B.N., Sagan, C., Bandurski, E.L., and Nagy, B. (1978). Ultraviolet-photoproduced organic solids synthesized under simulated Jovian conditions: Molecular analysis. *Science* *199*, 1199-1201.

Khare, B.N., Sagan, C., Zumberge, J.E., Sklarew, D.S., and Nagy, B. (1982). Organic solids produced by electrical discharge in reducing atmospheres: Tholin molecular analysis. *Icarus* *48*, 290-297.

Khare, B.N., Sagan, C., Shrader, S., and Arakawa, E. (1982). Molecular analysis of tholins produced under simulated Titan conditions. *Bull. Amer. Astron. Soc.*, in press.

Koch, E.E., and Skibowski, M. (1971). Optical absorption of gaseous methane, ethane, propane, and butane and reflection of solid methane and ethane in the vacuum ultraviolet. *Chem. Phys. Letts.* *9*, 429-432.

Krimigis, S.M., Armstrong, T.P., Axford, W.I., Bostrom, C.O., Gloeckler, G., Keath, E.P., Lanzerotti, L.J., Carbary, J.F., Hamilton, D.C., and Roelof, E.C. (1981). Low-energy charged particles in Saturn's magnetosphere: Results from Voyager 1. *Science* *212*, 225-231.

Krimigis, S.M., Armstrong, T.P., Axford, W.I., Bostrom, C.O., Gloeckler, G., Keath, E.P., Lanzerotti, L.J., Carbary, J.F., Hamilton, D.C., and Roelof, E.C. (1982). Low-energy hot plasma and particles in Saturn's magnetosphere. *Science* *215*, 571-577.

Krimigis, S.M., Armstrong, T.P., Axford, W.I., Bostrom, C.O., Fan, C.Y., Gloeckler, G., and Lanzerotti, L.J. (1977). The low energy charged particle (LECP) experiment on the Voyager spacecraft. *Space Sci. Rev.* *21*, 329-354.

Kuiper, G.P. (1944). Titan: A satellite with an atmosphere. *Astrophys. J.* *100*, 378-383.

Kunde, V.G., Aikin, A.C., Hanel, R.A., Jennings, D.E., Maguire, W.C., and Samuelson, R.E. (1981). C_4H_2, HC_3N and C_2N_2 in Titan's atmosphere. *Nature* *292*, 686-688.

Macy, W.W. (1973). Doctoral thesis, Princeton University.

Maguire, W.C., Hanel, R.A., Jennings, D.E., Kunde, V.G., and Samuelson, R.E. (1981). C_3H_8 and C_3H_4 in Titan's atmosphere. *Nature* *292*, 683-686.

Maguire,, W.C., Hanel, R., Jennings, D., Samuelson, R., Aikin, A., and Yung, Y. (1982). CO_2 on Titan. (Presented at Saturn Conference, Univ. Arizona, May 14, 1982.)

Ness, N.F., Acuna, M.H., Lepping, R.P., Connerney, J.E.P., Behannon, K.W., Burlaga, L.F., and Neubauer, F.M. (1981). Magnetic field studies by Voyager 1: Preliminary results at Saturn. Science 212, 211-217.

Ness, N.F., Acuna, M.H., Behannon, K.W., Burlaga, L.F., Connerney, J.E.P., Lepping, R.P., and Neubauer, F.M.(1982). Magnetic field studies by Voyager 2: Preliminary results at Saturn. Science 215, 558-563.

Okabe, H., and Becker, D.A. (1963). Vacuum ultraviolet photochemistry. VII. Photolysis of n-butane. J. Chem. Physics 39, 2549-2555.

Rages, K., and Pollack, J.B. (1983). Vertical distribution of scattering hazes in Titan's upper atmosphere. Preprint.

Raulin, F., Bossard, A., Toupance, G., and Ponnamperuma, C. (1979). Abundance of organic compounds photochemically produced in the atmospheres of the outer planets. Icarus 38, 358.

Sagan, C. (1971). The solar system beyond Mars: an exobiological survey. Space Sci. Rev. 11, 73-112.

Sagan, C. (1973). The greenhouse of Titan. Icarus 18, 649-656.

Sagan, C. (1974). Organic chemistry in the atmosphere. In The Atmosphere of Titan (D.M. Hunten, Ed.). NASA Special Publication SP-340, Washington D.C.

Sagan, C., and Khare, B.N. (1971a). Long wavelength photoproduction of amino acids on the primitive Earth. Science 173, 417-420.

Sagan, C., and Khare, B.N. (1971b). Experimental jovian photochemistry: Initial results. Astrophys. J. 168, 563-570.

Sagan, C., and Khare, B.N. (1974). Unpublished experiments.

Sagan, C., and Khare, B.N. (1973). Experimental interstellar organic chemistry: Preliminary findings. In Molecules in the Galactic Environment (M. Gordon and L. Snyder, Eds.), pp. 399-408. John Wiley, New York.

Sagan, C., and Khare, B.N. (1981). The organic clouds of Titan. Bull. Amer. Astron. Soc. 13, 701.

Sagan, C., and Khare, B.N. (1982). The organic clouds of Titan. Origins of Life, in press.

Samuelson, R.E., Hanel, R.A., Kunde, V.G., Maguire, W.C. (1981). Mean molecular weight and hydrogen abundance of Titan's atmosphere. Nature 292, 688-693.

Scattergood, T., and Owen, T. (1977). On the sources of ultraviolet absorption in spectra of Titan and the outer planets. Icarus 30, 780-788.

Smith, B.A., Soderblom, L., Beebe, R., Boyce, J., Briggs, G., Bunker, A., Collins, S.A., Hansen, C.J., Johnson, T.V., Mitchell, J.L., Terrile, R.J., Carr, M., Cook, A.F., II, Cuzzi, J., Pollack, J.B., Danielson, G.E., Ingersoll, A., Davies, M.E., Hunt, G.E., Masursky, H., Shoemaker, E., Morrison, D., Owen, T., Sagan, C., Veverka, J., Strom, R., and Suomi, V.E. (1981). Encounter with Saturn: Voyager 1 imaging science results. Science 212, 163-190.

Smith, B.A., Soderblom, L., Batson, R., Bridges, P., Inge, J., Masursky, H., Shoemaker, E., Beebe, R., Boyce, J., Briggs, G., Bunker, A., Collins, S.A., Hansen, C.J., Johnson, T.V., Mitchell, J.L., Terrile, R.J., Cook, A.F., II, Cuzzi, J., Pollack, J.B., Danielson, G.E., Ingersoll, A.P., Davies, M.E., Hunt, G.E., Morrison, D., Owen, T., Sagan, C., Veverka, J., Strom, R., and Suomi, V.E. (1982a). A new look at the Saturn system: the Voyager 2 images. Science 215, 504-537.

Smith, E.J., Davis, L., Jr., Jones, D.E., Coleman, P.J., Jr., Colburn, D.S., Dyal, P., and Sonett, C.P. (1980). Saturn's magnetic field and magnetosphere. Science 207, 407-410.

Smith, G.R., Strobel, D.F., Broadfoot, A.L., Sandel, B.R., Shemansky, D.E., and Holberg, J.B. (1982b). Titan's upper atmosphere: Composition and temperature from the EUV solar occulation results. J. Geophys. Res. 87, 1351-1359.

Sromovsky, L.A., Suomi, V.E., Pollack, J.B., Krauss, R.J., Limaye, S.S., Owen, T., Revercomb, H.E., and Sagan, C. (1981). Implications of Titan's north-south brightness asymmetry. Nature 292, 698-702.

Strobel, D.F. (1974). The photochemistry of hydrocarbons in the atmosphere of Titan. Icarus 21, 466-470.

Strobel, D.F. (1982). Chemistry and evolution of Titan's atmosphere. (Preprint.)

Toon, O.B., Turco, R.P., and Pollack, J.B. (1980). A physical model of Titan's clouds. Icarus 43, 260-282.

Toupance, G., Raulin, F., Buvet, R. (1975). Formation of prebiochemical compounds in models of the primitive Earth's atmosphere. I: CH_4-NH_3 and CH_4-N_2 Atmospheres. Origins of Life 6, 83-90.

Trafton, L.M. (1972). The bulk composition of Titan's atmosphere. Astrophys. J. 175, 295-306.

Trafton, L.M. (1973). Titan's spectrum and atmospheric composition. In The Atmosphere of Titan (D. Hunten, Ed.). NASA Special Publication SP-340, Washington, D.C.

Tyler, G.L., Eshleman, V.R., Anderson, J.D., Levy, G.S., Lindal, G.F., Wood, G.E., Croft, T.A. (1981). Radio science investigations of the Saturn system with Voyager 1: Preliminary results. Science 212, 201-206.

van Allen, J.A., Thomsen, M.F., Randall, B.A., Rairden, R.L., and Grosskrentz, C.L. (1980). Saturnian trapped radiation and its absorption by satellites and rings: The first results from Pioneer. Science 207, 411-421.

Veverka, J. (1973). Titan: Polarimetric evidence for an optically thick atmosphere? Icarus 18, 657-660.

Weast, R.C., Ed. (1980). CRC Handbook of Chemistry and Physics, 61st Ed. CRC Press, Boca Raton, FL.

Wolfe, J.H., Mihalov, J.D., Collard, H.R., McKibbin, D.D., Frank, L.A., and Intriligator, D.S. (1980). Preliminary results on the plasma environment of Saturn from the Pioneer 11 plasma analyzer experiment. Science 207, 403-407.

Yung. Y. (1982). Private communication.

Zellner, B. (1973). The polarization of Titan. Icarus 18, 661-664.